nature communications

Article

https://doi.org/10.1038/s41467-024-51442-2

# The TGFβ type I receptor kinase inhibitor vactosertib in combination with pomalidomide in relapsed/refractory multiple myeloma: a phase 1b trial

Received: 30 January 2024

Accepted: 7 August 2024

Published online: 27 August 2024

Check for updates

Ehsan Malek[1,2,3] ✉, Priyanka S. Rana[1,2,3], Muthulekha Swamydas[1,2,3], Michael Daunov[1,2,3], Masaru Miyagi[3,4,5], Elena Murphy[6], James J. Ignatz-Hoover[1,2,3], Leland Metheny[1,2,3], Seong Jin Kim[7] & James J. Driscoll[1,2,3] ✉

Functional blockade of the transforming growth factor-beta (TGFβ) signalling pathway improves the efficacy of cytotoxic and immunotherapies. Here, we conducted a phase 1b study (ClinicalTrials.gov., NCT03143985) to determine the primary endpoints of safety, tolerability, and maximal tolerated dose (200 mg twice daily) for the orally-available TGFβ type I receptor kinase inhibitor vactosertib in combination with pomalidomide in relapsed and/or refractory multiple myeloma (RRMM) patients who had received ≥2 lines of chemoimmunotherapy. Secondary endpoints demonstrated sustained clinical responses, favorable pharmacokinetic parameters and a 6-month progression-free survival of 82%. Vactosertib combined with pomalidomide was well-tolerated at all dose levels and displayed a manageable adverse event profile. Exploratory analysis indicated that vactosertib co-treatment with pomalidomide also reduced TGFβ levels in patient bone marrow as well as the level of $CD8^+$ T-cells that expressed the immunoinhibitory marker PD-1. In vitro experiments indicated that vactosertib+pomalidomide co-treatment decreased the viability of MM cell lines and patient tumor cells, and increased $CD8^+$ T-cell cytotoxic activity. Vactosertib is a safe therapeutic that demonstrates tumor-intrinsic activity and can overcome immunosuppressive challenges within the tumor microenvironment to reinvigorate T-cell fitness. Vactosertib offers promise to improve immunotherapeutic responses in heavily-pretreated MM patients refractory to conventional agents.

Multiple myeloma (MM) is a genetically heterogeneous hematologic malignancy characterized by the excessive proliferation of clonal plasma cells[1,2]. MM is a treatable but generally incurable disease in which a small proportion of patients can achieve long-term remission[3]. Treatment of MM presents unique challenges due to the complex genetic heterogeneity and molecular pathophysiology[4,5]. Given that MM is the second most common blood cancer and characterized by cycles of remission and relapse, the development of new therapeutic modalities is crucial[6,7]. The prognosis for MM patients has improved substantially over the past two decades with the development of more

A full list of affiliations appears at the end of the paper. ✉e-mail: ehsan.malek@RoswellPark.org; james.driscoll@UHhospitals.org

effective therapeutics, e.g., proteasome inhibitors, and regimens that demonstrate greater anti-tumor activity[8–10]. Management of relapsed and/or refractory disease represents a critical aspect of the overall care for MM patients and is at the forefront of scientific and clinical research[10–12].

Over the past 2 decades, the myeloma community has witnessed the success of immunomodulatory drugs (IMiDs), monoclonal antibodies, chimeric antigen receptor (CAR) T-cells and bispecific T-cell engagers (BiTEs) to reengage the immune system and break the *circulus vitiosus* of tumor-induced immunosuppression[13,14]. IMiDs are widely used as primary and maintenance therapy and resistance to prior lenalidomide (Revlimid) or pomalidomide (Pomalyst) treatment is a major patient classification feature. However, nearly all patients ultimately relapse through molecular mechanisms that remain elusive, even those who achieve a minimal residual disease (MRD)$^{neg}$ status and a complete remission to initial therapy.

The TGFβ1 signaling pathway promotes cancer progression by concomitantly enhancing tumor growth, drug resistance and metastases while inhibiting the host immune response[15,16]. TGFβ1 signals through type I (TβRI) and type II (TβRII) receptors by directly phosphorylating the downstream transcription factors Smad2/Smad3[17]. While malignant plasma cells are not known to harbor mutations in the TGFβ pathway, increased levels of secreted TGFβ1 from myeloma and bone marrow (BM) stromal cells impair immune surveillance and promote disease progression. Elevated levels of TGFβ1 in the sera of MM patients correlate with drug resistance, tumor progression and poor prognosis[18].

Here, we hypothesized that inhibition of the TGFβ1 signaling pathway represents a viable strategy to treat RRMM patients since TGFβ1 promotes the development of drug resistance and myeloma growth. Vactosertib (TEW-7197, Medpacto, Seoul, Republic of Korea) is a selective inhibitor of the serine/threonine TβRI receptor kinase (ALK5) that suppresses tumor progression and metastatic growth in preclinical models of cancer[19,20]. While the effects of TGFβ1 on tumor cells are varied and context-specific, its role in immune evasion within the tumor microenvironment (TME) appears similar across multiple cancer types since TGFβ1 is a central mediator of immune tolerance[21–24]. Vactosertib has been shown to inhibit the Smad/TGFβ signaling pathway, cell migration, invasion, and lung metastasis in MMTV/c-Neu mice and 4T1 orthotopic-grafted mice[25]. Combination of vactosertib with the PRMT5 inhibitor T1-44 inhibited tumor invasion and prolonged survival in a murine model of pancreatic cancer[26]. In addition, oral treatment with the ALK5 inhibitor, EW-7197 (2.5 mg/kg daily) suppressed melanoma progression and enhanced cytotoxic T-lymphocyte (CTL) responses[27]. These observations led us to determine the safety and efficacy of vactosertib in RRMM patients and to test the hypothesis that disrupting TGFβ1 signaling can overcome immunosuppression.

## Results

### Trial design, Swimmer's and Waterfall plots to evaluate patient response to vactosertib and pomalidomide

Patients enrolled in the phase 1b dose escalation cohort received vactosertib plus pomalidomide as shown (Fig. 1a). Median patient age was 68 years (range 55–77), two patients (10%) were ≥75 years of age and four patients (20%) had high-risk disease (Table 1). The majority of patients were White ($N = 13$, 65%), six (30%) self-identified as Black/African-American, one self-identified as Asian (5%) and most were male ($N = 12$, 60%). All patients had previously received a proteasome inhibitor and IMiD. Most patients had an Eastern Cooperative Oncology Group (ECOG) score of one ($N = 14$, 70%) while six had a score of 0 (30%). Most patients had IgG-specific disease ($N = 14$, 70%), five had IgA disease (25%) and one had light chain (LC) disease (5%). Three patients (15%) had received one prior line of therapy, 11 (55%) had received two lines of therapy, 4 (20%) had received three lines of therapy and 2 (10%) had received four lines of therapy. Most patients also had undergone autologous stem cell transplant (ASCT) ($N = 14$; 70%). Best responses to prior treatment were SD ($N = 1$; 5%); PR ($N = 6$; 30%); VGPR ($N = 5$; 25%); CR ($N = 6$; 30%) and PD ($N = 2$; 10%).

Patients were treated with vactosertib at one of four dose levels (Fig. 1a). Dose level I was 60 mg po qd; level II was 120 mg po qd; level III 100 mg po bid; and level IV was 200 mg po bid. Vactosertib was administered on days 1–5, 8–12, 15–19, 22–26 of 28-day cycles. Patients were simultaneously treated with pomalidomide administered at 4 mg po qd on days 1–21. Three patients were accrued at dose levels I–IV before going to the extension cohort. Vactosertib combined with pomalidomide induced durable responses with 82% PFS-6 at 6 months as estimated by Kaplan–Meier analysis, while historically treatment with pomalidomide alone achieved only 20% PFS-6 (Fig. S1). Patients were included in drug safety and toxicity, preliminary activity analyses, pharmacokinetics (PK) determination, and correlative translational and immunologic studies.

The total number of grades 1–5 adverse events (AEs) by dose level is shown (Table S1). A single grade 4 elevated bilirubin (5%) and a single grade 4 elevated lipase (5%) were observed as well as four grade 4 events of decreased neutrophils (20%). The frequency of other grade 3 or higher non-hematological treatment-emergent AEs was generally low (Table S2). A grade 3 decrease in white blood cells was observed in 11 (55%), 7 (35%), and 6 (30%) patients, respectively. Common AEs of grade 3 were clinically manageable. Dose-limiting toxicities (DLTs) in the overall patient population were limited following oral administration of vactosertib at all dose levels as well as in the dose extension cohort tested (200 mg po bid). A serious treatment-emergent event (grade 4 hepatotoxicity) was reported in one patient (5%) as a DLT (Table S3). There were no deaths from AEs possibly related to treatment within 30/90 days of treatment and one death from myeloma progression. Therefore, 200 mg po bid was defined as the maximum tolerated dose (MTD). Based upon International Myeloma Working Group (IMWG) criteria, four patients demonstrated a partial response (PR), four had a minimal response (MR), seven had stable disease (SD) and five had disease progression (Fig. 1b, Table S4)[28]. Swimmer's plot indicated that two patients who received 12 cycles of vactosertib combined with pomalidomide had PRs. A waterfall plot indicated an increase in the biochemical marker of disease (M-spike or LC level) correlated with disease progression, while a reduction in biochemical marker correlated with PR, MR or SD (Fig. 1c). The median time to response for all patients and responders was eight weeks and median duration of response was ~12 weeks. Based upon the clinical benefit rate (CBR), 15 of 20 patients (75%) demonstrated clinical benefit (Table S4) and clinical benefit was observed at all dose levels.

PK properties of vactosertib following oral administration were well-characterized by a two-compartment model with parallel first-order and Michaelis–Menten elimination and approximated target-mediated drug disposition kinetics (Table S5)[29]. $T_{max}$ at 100 mg was observed at 1.3 ± 0.5 h, and at 200 mg observed at 1.5 ± 1.0 h. The half-life ($t_{1/2}$) after 100 mg administration was 3.5 ± 0.4 h and after 200 mg administration was 3.3 ± 1.3 h. The $AUC_{obs}$ was 6175.5 ± 1349.7 ng/ml h after administration of 100 mg vactosertib and 4251.8 ± 1307.6 ng/ml h after administration of 200 mg vactosertib. Vactosertib PKs had previously been assessed by nonlinear mixed-effects modeling of plasma concentration-time data obtained from a phase 1 trial conducted in patients with advanced solid tumors[20,29,30]. The observed half-life of 3.5 h was comparable to the value (3.0 h) determined in a recent phase I trial of vactosertib in combination with paclitaxel as second-line treatment in metastatic gastric adenocarcinoma[31].

### Effect of TGFβ1, vactosertib and pomalidomide on canonical and non-canonical TGFβ-signaling in MM cells

Based upon the clinical success of vactosertib in combination with pomalidomide, we sought to address the mechanism of anti-myeloma activity for vactosertib alone and combined with pomalidomide.

https://doi.org/10.1038/s41467-024-51442-2

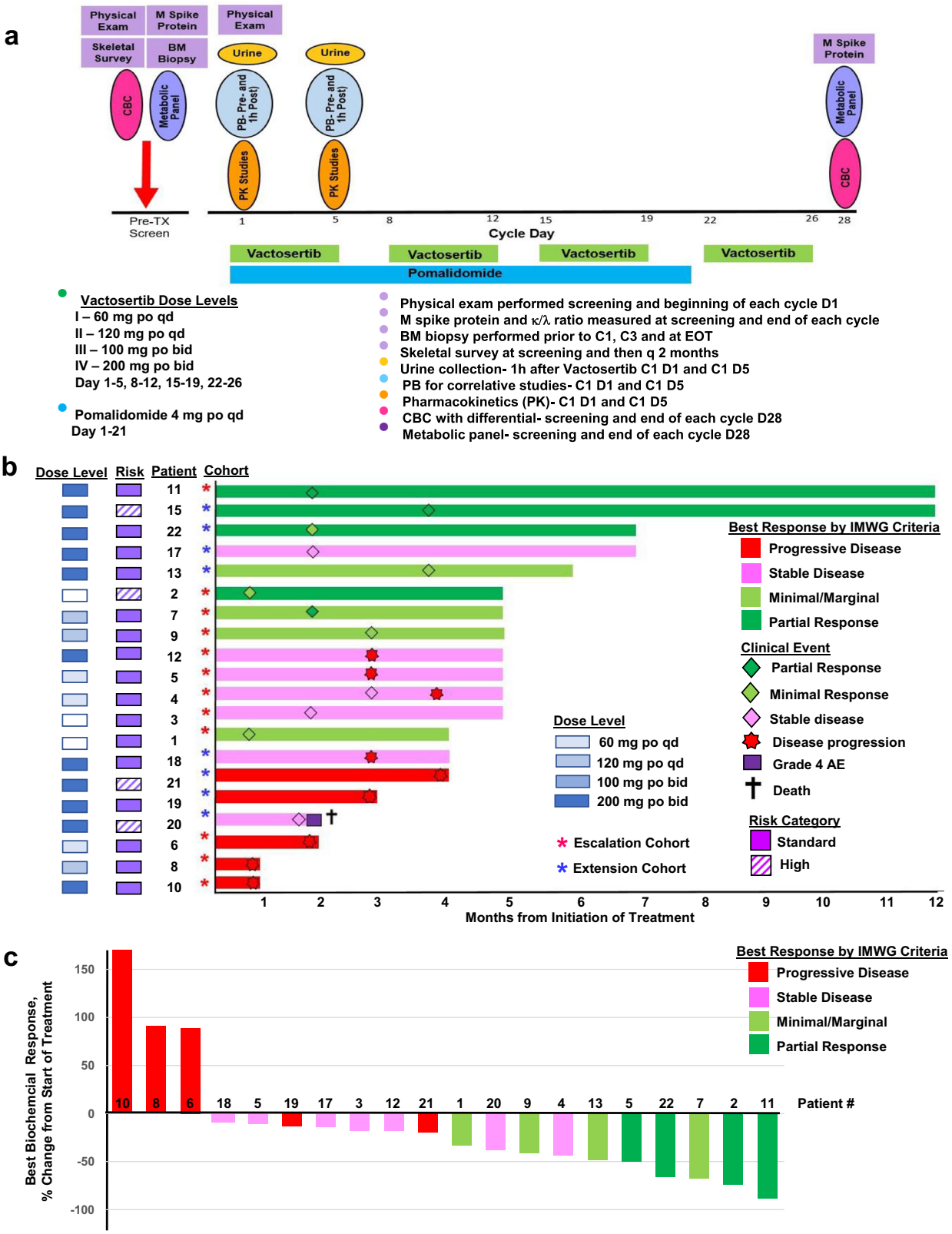


**Fig. 1 | Trial design, Swimmer's plot and Waterfall plot to evaluate the response of patients to vactosertib and pomalidomide. a** Vactosertib and pomalidomide dose administration schedule and vactosertib dose levels for the phase 1b dose escalation cohort. Also shown is the schedule for clinical and laboratory testing. **b** Swimmer's plot indicates the individual trajectories and outcomes over the study duration in the 20 patients that received full-dose treatment. The magnitude of the *Y*-axis value for each patient indicates the months of study from the initiation of treatment. The color attributed to each patient's lane in the Swimmer's plot correlates with the response based upon IMWG criteria. **c** Waterfall plot indicates the maximal change in baseline of the biochemical marker, i.e., M-spike or LC, value for the same 20 patients as in (**b**). The magnitude of the vertical bar for each patient represented in the Waterfall represents the best change in the biochemical marker measured from the initiation of treatment. The color attributed to the vertical bar indicates with the patient response to treatment based upon IMWG criteria.

https://doi.org/10.1038/s41467-024-51442-2

**Table 1 | Patient baseline characteristics and treatment responses**

| | | |
|---|---|---|
| **Sex** | Female | 8 (40%) |
| | Male | 12 (60%) |
| **Race** | White | 13 (65%) |
| | Black/AA | 6 (30%) |
| | Asian | 1 (5%) |
| | Other | 0 (0%) |
| **Age, years** | Median | 68 (range 55–77) |
| **ECOG** | 0 | 6 (30%) |
| | 1 | 14 (70%) |
| **Disease type** | IgG | 14 (70%) |
| | IgA | 5 (25%) |
| | IgM | 0 (0%) |
| | LC | 1 (5%) |
| **ISS score at diagnosis** | 1 | 3 (15%) |
| | 2 | 8 (40%) |
| | 3 | 7 (35%) |
| | Unknown | 2 (10%) |
| **Cytogenetic risk at initial diagnosis** | High | 5 (25%) |
| | Low | 15 (75%) |
| **Prior systemic lines of therapy** | 1 | 3 (15%) |
| | 2 | 11 (55%) |
| | 3 | 4 (20%) |
| | 4 | 2 (10%) |
| **Prior therapies** | Proteasome inhibitor | 20 (100%) |
| | IMiD | 20 (100%) |
| | Melphalan | 14 (70%) |
| **Previous ASCT** | | 14 (70%) |
| **Median prior lines of therapy** | 2 | |
| **Best response to prior treatment** | | |
| Stable disease (SD) | 1 | (5%) |
| Minor response | 0 | (0%) |
| Partial response (PR) | 6 | (30%) |
| Very good partial response (VGPR) | 5 | (25%) |
| Complete response | 6 | (30%) |
| Progressive disease | 2 | (10%) |

Summary of baseline characteristics by demographics, prior treatment regimen and prior response to therapy. Cytogenetic risk was considered high risk (HR) based upon the *t*(4;14), *t*(14;16) and *t*(14;20) translocations that have been associated with poor prognosis, and their presence identifies HR disease. On the other hand, patients with *t*(11;14), *t*(6;14) and/or trisomies are considered to have standard-risk (SR) disease. PIs refers to the proteasome inhibitors bortezomib (Velcade), carfilzomib (Kyprolis), and ixazomib (Ninlaro). IMiD refers to the immunomodulatory drugs thalidomide (Thalidomid), lenalidomide (Revlimid), and pomalidomide (Pomalyst). Data are presented as *n* (%).

Moreover, while IMiDs have markedly improved the treatment of MM patients, IMiD resistance commonly underlies relapse of disease and develops through molecular mechanisms that remain elusive[32]. We initially probed the anti-myeloma intrinsic activity of vactosertib relative to pomalidomide and lenalidomide. Drugs were added at indicated concentrations and the effect on the viability of patient CD138$^+$ cells determined (Fig. S2). Vactosertib reduced cell viability in a dose-dependent manner, and the effect appeared greater than that observed with either IMiD.

We next probed the effects of vactosertib and pomalidomide alone and in combination on TGFβ-driven canonical (SMAD-dependent) and non-canonical (SMAD-independent) pathways. TGFβ is a multifunctional cytokine that mediates a number of complex responses that contribute to tumorigenesis by recruiting and activating the transcription factors SMAD2/3. The TGFβRII subunit binds TGFβ1 and recruits the subunit into a heterotetrameric complex. TGFβRI is activated upon phosphorylation by TGFβRII and phosphorylates downstream effectors to transduce signals. Canonical TGFβ-driven signaling activates SMAD2/3 nuclear translocation and regulates transcription, while non-canonical TGFβ signaling involves extracellular signal-regulated kinase (ERK)/mitogen-activated protein kinase (MAPK) signaling[33]. Western blotting indicated that treatment of MM1.S cells with TGFβ1 increased the phosphorylation of both canonical (SMAD2/3) and non-canonical (ERK1/2) pathway effectors (Fig. 2a; Fig. S1a). Treatment of MM1.S cells with vactosertib nearly completely eliminated SMAD2/3 phosphorylation in the presence of TGFβ1, However, vactosertib treatment also increased ERK1/2 phosphorylation, indicative of SMAD-independent receptor tyrosine kinase (RTK)-driven signaling. Importantly, pomalidomide treatment slightly reduced the phosphorylation of SMAD2/3 as well as ERK1/2 phosphorylation. Vactosertib treatment of other MMCLs, that are relatively resistant to pomalidomide and lenalidomide, also reduced SMAD2/3 phosphorylation (Fig. S4).

IMiDs are thalidomide analogs that possess pleiotropic anti-myeloma properties, e.g., immune modulation, anti-angiogenic, anti-inflammatory and anti-proliferative effects[34]. IMiDs are a cornerstone of treatment for MM patients and are used in therapeutic combinations at all stages of disease. The ubiquitously expressed protein cereblon (CRBN) is a substrate adapter subunit for the DDB1–Cul4–Rbx1–CRBN ($CRL4^{CRBN}$) E3 ubiquitin (Ub) ligase and the primary teratogenic target of pomalidomide[35,36]. Pomalidomide co-opts and enhances CRBN E3 Ub ligase activity to selectively enhance the degradation of the zinc-finger B-cell transcription factors IKZ1 and IKZ3, leading to cell death. As expected, the treatment of MM1.S cells with pomalidomide increased expression of cereblon and reduced the levels of IKZF1 and IKZF3 (Fig. 2a).

Co-treatment of MM1.S cells with vactosertib and pomalidomide increased cereblon levels and significantly reduced phospho-SMAD2/3 levels as well as phospho-ERK1/2, IKZF1 and IKZF3 levels (Fig. 2b). Importantly, the effects of vactosertib and pomalidomide on phospho-SMAD2/3 and phospho-ERK1/2 levels when added together were observed at concentrations lower than that observed when each drug was added individually.

### Phospho-ERK1/2 and Bcl-2 are upregulated in MM cells with acquired pomalidomide resistance

To further probe the effect of vactosertib in pomalidomide resistance, MM1.S cells were cultured in media containing successively increased concentrations of pomalidomide as a model of acquired pomalidomide resistance (Fig. S5). Western blotting indicated that the levels of phospho-SMAD2/3 and phospho-ERK1/2 were greater in pomalidomide-resistant MM1.S cells relative to parental cells (Fig. 3a; Fig. S6). Phosphorylation of ERK1/2 increases Bcl-2 levels to promote tumor cell proliferation and survival. Western blotting indicated that the pomalidomide-resistant MM1.S cells contained significantly elevated levels of phospho-ERK1/2 and Bcl-2.

MM1.S parental and pomalidomide-resistant cells were then treated with vactosertib and pomalidomide at the indicated concentrations and the effect on cell viability was determined (Fig. 3b). Results indicated that pomalidomide reduced the viability of parental cells with an $IC_{50}$~0.3 μM while pomalidomide-resistant cells exhibited an $IC_{50}$ of ~1.6 μM. Vactosertib reduced the viability of both MM1.S parental and pomalidomide-resistant cells with $IC_{50}$~1.5 μM. MM1.S parental and pomalidomide-resistant cells were then co-treated with vactosertib and pomalidomide at the indicated concentrations (Fig. 3c). Parental and pomalidomide-resistant cells were generally insensitive to vactosertib at concentrations ≤0.8 μM. Parental cells

https://doi.org/10.1038/s41467-024-51442-2

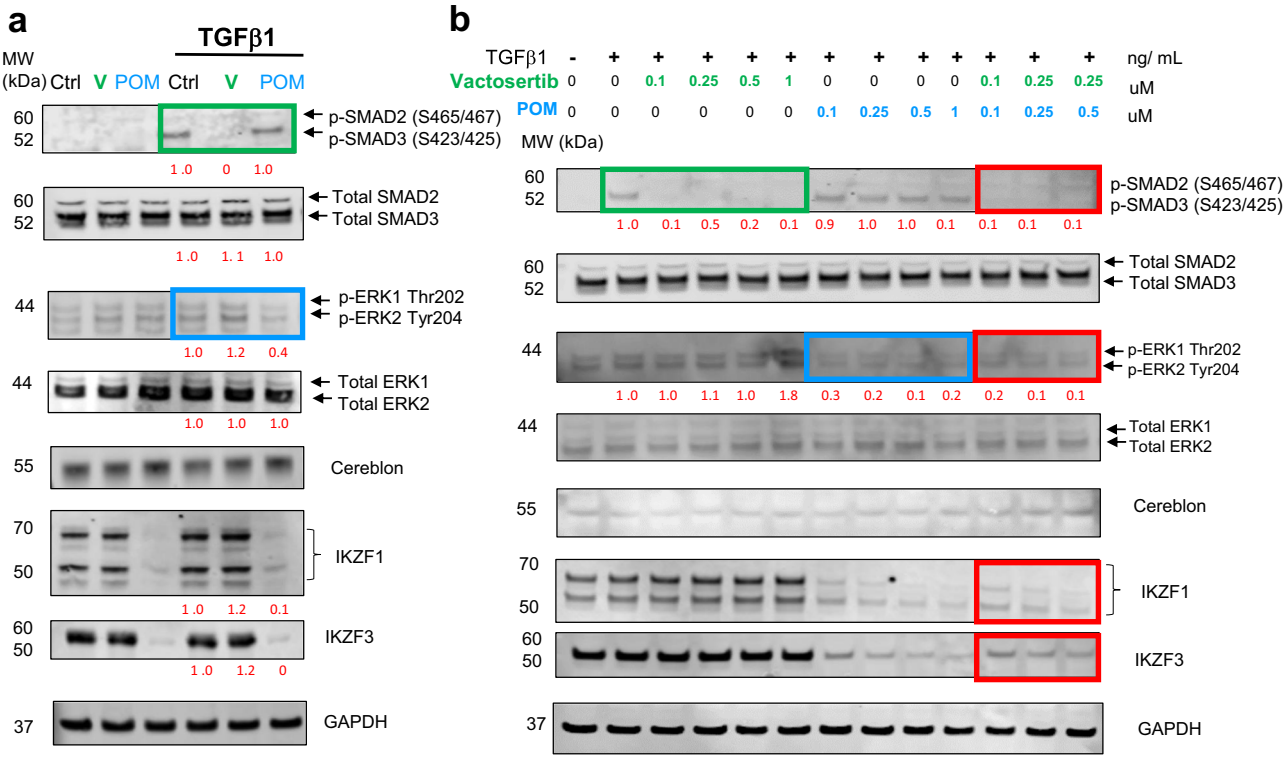


**Fig. 2 | Effect of TGFβ1, vactosertib and pomalidomide on canonical and non-canonical TGFβ-signaling in MM cells. a** Representative western blots of lysates from MM.1S cells treated with vactosertib (1 μM) or pomalidomide (1 μM) for 18 h with or without TGFβ1 (10 ng/mL) included in the culture media. Whole cell lysates were prepared and probed with the following antibodies: phospho-SMAD2/3, total SMAD2/3, phospho-ERK1/2, total ERK1/2, cereblon, IKZF1, IKZF3 and GAPDH. The densitometric values for total SMAD2/3 and total ERK1/2 are relative that the values measured in the presence of TGFβ and in the absence of vactosertib and pomalidomide. Densitometric values for phospho-SMAD2/3 with each treatment represent the value determined in the presence of TGFβ relative to the total SMAD2/3 value with the same treatment. Similarly, the value for phospho-ERK1/2 with each treatment represent the value determined in the presence of TGFβ relative to the total SMAD2/3 value with the same treatment. **b** Representative western blot of MM.1S cells treated with vactosertib or pomalidomide individually and in combination at the indicated concentrations for 18 h in the presence of TGFβ1 (10 ng/mL). Experiments were independently performed twice. Whole cell lysates were collected and probed with the same antibodies as above. Source data are provided as a Source Data file.

were insensitive to pomalidomide at concentrations ≤0.2 μM, while pomalidomide-resistant cells were sensitive to the drug only at concentrations >1.0 μM. However, the combination of vactosertib with pomalidomide significantly reduced the viability of pomalidomide-resistant cells at drug concentrations that were ineffective as monotherapy. MM1.S parental and pomalidomide-resistant cells were then treated with vactosertib at 0.8 μM (which alone did not reduce the viability of parental or drug-resistant cells) and pomalidomide at low doses (0.1 and 0.2 μM). Results indicated that co-treatment with vactosertib and pomalidomide overcame drug resistance. Similar results were observed using patient BM-derived CD138$^+$ cells (Fig. 3c).

## Synergistic effect of vactosertib and pomalidomide on apoptosis in MM cells

Pomalidomide-resistant cells were treated with vactosertib and pomalidomide, lysates prepared and probed by western blot. Results indicated a significant decrease in the levels of phospho-ERK1/2 and Bcl-2 as well as an increase in the level of cleaved caspase-3 (Fig. 4a). Co-treatment of parental and pomalidomide-resistant MM1.S cells and patient BM-derived CD138$^+$ cells with vactosertib and pomalidomide also increased the relative percent of annexin-V+ cells (Fig. 4b, c).

## Effect of TGFβ1, vactosertib and pomalidomide on the myeloma immunophenotype

To determine the effect of vactosertib on the antigenicity of MM cells, we screened cell surface marker expression using a monoclonal antibody panel that detects 242 proteins. Screening allowed us to quantify the effect of cytokine or drug treatment on the expression of immunogenic markers and shed light on potential actionable markers. TGFβ1 treatment increased the level of CD1a, CD36, CD79, CD77, and integrin β7 on RPMI-8226 cells (Fig. S7a). In the presence of TGFβ1, vactosertib treatment upregulated the expression of 15 cell surface makers more than twofold, including HLA-ABC (Fig. 5a). Pomalidomide upregulated 35 surface makers more than twofold, and also significantly increased the level of HLA-ABC (Fig. 5b). Combination of vactosertib and pomalidomide in the presence of TGFβ1 upregulated five cell surface markers. Importantly, vactosertib, combined with pomalidomide, upregulated HLA-ABC expression (Fig. 5c, d). TGFβ1 treatment downregulated 18 surface markers on RPMI-8226 cells relative to the untreated cells (Fig. S7b). Vactosertib reduced 11 surface markers, pomalidomide downregulated 29 markers and vactosertib combined with pomalidomide downregulated 13 markers (Fig. 5e–g). Importantly, vactosertib and pomalidomide, alone or combined, reduced expression of the immunoinhibitory receptor PD-L1 on MM cells.

## Effect of vactosertib and pomalidomide treatment on patient BM cytokines and cells

We next probed the systemic, tumor extrinsic effects of vactosertib on cytokines, immune and tumor cells present in patient BM. Latent TGFβ1 and interleukin (IL)-6 levels were not significantly changed in patient BM samples at the end of treatment (EOT) (Fig. 6a). However, free (active) TGFβ1 levels were significantly reduced in patient BM samples at the EOT. Immunostaining followed by flow cytometry did

https://doi.org/10.1038/s41467-024-51442-2

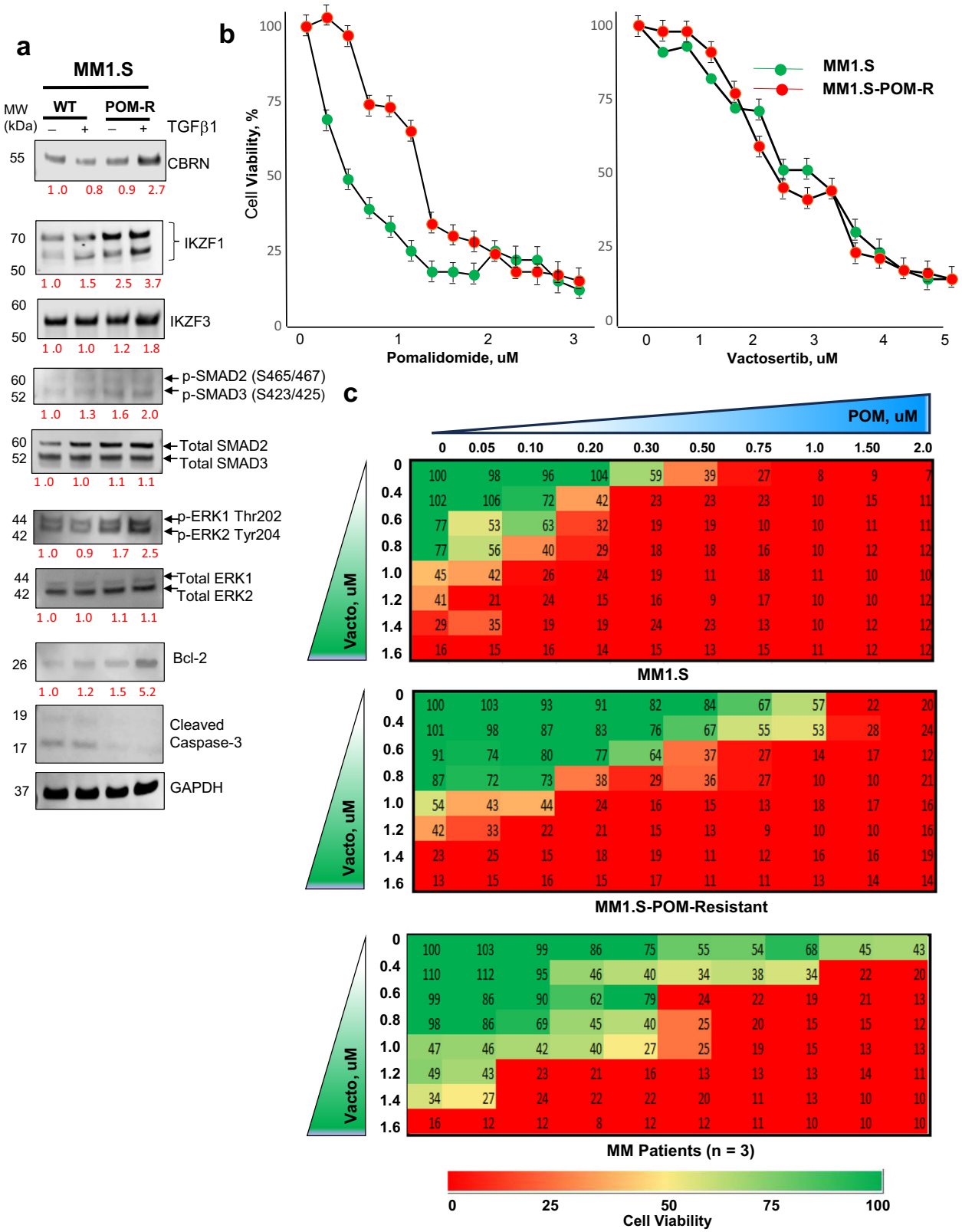


not detect statistically significant differences in the total number of individual cell types within the BM mononuclear cell (BMMC) fraction following treatment (Fig. S8). TGFβ1 supports T-cell development, homeostasis, tolerance and differentiation leading to functional diversity in the T-cell pool[37]. Therefore, we explored the immunophenotype of $CD8^+$ T-cells isolated from patient BM prior to and at the EOT. The immunosuppressive marker programmed cell death-1 (PD-1) is a member of the CD28 superfamily that delivers negative signals upon interaction with its ligands PD-L1 and PD-L2[38]. T-cell immunoglobulin and mucin domain-containing protein 3 (TIM-3) is expressed on IFN-γ-producing $CD4^+$ and $CD8^+$ T-cells, and B and T-lymphocyte attenuator (BTLA) is a CD28/B7 family member that shares structural and functional similarity with cytotoxic T-lymphocyte-associated protein 4 (CTLA-4)[39–42]. Results indicated that

**Fig. 3 | Effectors upregulated in MM cells with acquired pomalidomide resistance. a** Representative western blots of MM.1S and MM.1S-pomalidomide-resistant cells cultured with or without TGFβ1 (10 ng/mL) treatment. Whole cell lysates were prepared and probed with the antibodies indicated in Fig. 2, along with Bcl-2 and cleaved caspase. Densitometric values for cereblon, IKZF1 and IKZF3 are relative to the value determined in WT (parental) cells in the absence of TGFβ. Densitometric values for total SMAD2/3 and total phospho-ERK1/2 are relative that the values measured in the absence of TGFβ in WT (parental) cells. Densitometric values for phospho-SMAD2/3 were determined relative to the total SMAD2/3 value determined with the same cells (either WT or pomalidomide-resistant) with or without TGFβ. Similarly, densitometric values for phospho-ERK1/2 were determined relative to the total ERK1/2 value determined with the same cells (WT or pomalidomide-resistant) with or without TGFβ. Experiments were independently performed twice. **b** Shown is the dose-dependent effect of pomalidomide and vactosertib on MM1.S parental and pomalidomide-resistant cells. Cells were treated with drugs at each indicated concentrations in triplicate and viability then determined using the XTT assay. Values shown represent the arithmetic mean of three independent experiments. **c** Concentration dependent combined effect of vactosertib and pomalidomide on MM.1S parental, pomalidomide-resistant and patient CD138$^+$ cells. Cells were treated with drugs at each indicated concentrations in triplicate and viability then determined using the XTT assay. Values shown represent the arithmetic mean of three independent experiments. Green boxes indicate highest viability, yellow boxes intermediate viability and red boxes lowest viability. Source data are provided.

in vivo treatment of MM patients with vactosertib and pomalidomide led to a reduction in the levels of PD-1, TIM-3, BTLA and CTLA-4-expressing CD8$^+$ T-cells within the BMMC fraction (Fig. 6b).

### Vactosertib directly modulates the CD8$^+$ T-cell immunophenotype

We investigated the effect of vactosertib, alone and combined with pomalidomide, on CD8$^+$ T-cells isolated from healthy donors and RRMM patients. Physiologic doses of TGFβ1 added to healthy CD8$^+$ T-cells in culture increased PD-1 expression by 2.5-fold (Fig. 7a). Treatment of healthy T-cells with TGFβ1 alone did not increase TIM-3 or BTLA expression (CTLA-4 was not detected on healthy T-cells). Vactosertib, alone or combined with pomalidomide, significantly suppressed the effect of TGFβ1 on T-cell expression of PD-1, while pomalidomide in combination with vactosertib slightly increased BTLA expression. Next, CD8$^+$ T-cells isolated from MM patients were cultured with TGFβ1 combined with either vactosertib or pomalidomide alone, or with vactosertib combined with pomalidomide (Fig. 7b). TGFβ1 did not increase the level of PD-1 on patient CD8$^+$ T-cells, most likely because these cells had been isolated from the TGFβ1-rich TME. Vactosertib treatment of patient CD8$^+$ T-cells decreased PD-1 expression up to 40% and decreased TIM-3 expression by ~65%. In addition, vactosertib co-treatment with pomalidomide significantly reduced the expression of PD-1 and TIM-3 on CD8$^+$ T-cells from most patients. PD-1 binding to its ligand PD-L1 activates downstream signaling pathways that inhibit T-cell activation. Abnormally high PD-L1 expression on tumor cells and antigen-presenting cells within the TME mediates immune escape. Vactosertib significantly reduced PD-L1 and PD-L2 expression on RPMI-8226 cells. Vactosertib treatment, alone or combined with pomalidomide, reduced PD-L1 and PD-L2 expression on CD138$^+$ cells from the majority of patients (Fig. 7c, d). Vactosertib and pomalidomide, alone or combined, also reduced the amount of TGFβ1 detected in CD8$^+$ T-cell culture supernatants, while pomalidomide, alone or combined with vactosertib, reduced the level of TGFβ1 in CD138$^+$ cell culture supernatants (Fig. S9a–c).

### Vactosertib directly targets CD8$^+$ T-cells and promotes T-cell fitness

TGFβ is present within the TME to promote neoplastic progression and suppress T-cell immunosurveillance[43]. Observations of diminished in vitro CD8$^+$ T-cell cytolytic activity in the presence of TGFβ provided early evidence for TGFβ-mediated inhibition of T-cell responses[44]. This effect is primarily due to the inhibitory effects of TGFβ on T-cell fitness, i.e., proliferation and cytolytic activity. We queried whether vactosertib modulated the effect of TGFβ on T-cell activity and fitness. TGFβ slightly reduced the viability of patient CD8$^+$ T-cells, while vactosertib suppressed the TGFβ effect (Fig. 8a, b). CD8$^+$ T-cells mediate direct killing of tumor cells through the production of cytokines, e.g., interferon-γ (IFN-γ) and tumor necrosis factor-α (TNF-α). In the presence of TGFβ, vactosertib increased the amounts of TNF-α and IFN-γ detected in culture supernatants (Fig. 8c, d). Patient CD138$^+$ cells were co-cultured with autologous CD8$^+$ T-cells and flow cytometry results indicated a low percentage of annexin$^+$ CD138$^+$ cells. However, treatment of CD138$^+$ cells with vactosertib, alone or combined with pomalidomide, followed by co-culture with CD8$^+$ T-cells significantly increased the percentage of annexin$^+$/CD138$^+$ cells (Fig. 8e).

## Discussion

Here we report a prospective analysis to demonstrate the safety, tolerability and efficacy of the TβRI kinase inhibitor vactosertib in combination with pomalidomide to treat RRMM, a population with an important unmet medical need. Patients included in our study represent a cohort with limited remaining treatment options. The proportion of patients that underwent previous ASCT ($N = 14$, 70%) and the older age of patients included in the present study closely reflects the population of patients with RR disease. However, our results suggest that treatment with oral vactosertib in combination with pomalidomide was well-tolerated, even in transplant-ineligible and elderly patients. The overall response rate (ORR) of 30% (partial + minimal response) in efficacy-evaluable patients treated with vactosertib and pomalidomide exceeded ORRs reported for other agents evaluated to treat RRMM[45,46]. For example, the first-in-class peptide-drug conjugate melphalan flufenamide (melflufen) targets aminopeptidases to rapidly and selectively release alkylating agents into tumor cells. Melphalan flufenamide plus dexamethasone demonstrated an ORR of 31% in the phase II HORIZON trial in RRMM patients[45]. Similarly, in the phase 3 MM-003 study, the ORR after a median follow-up of 10.0 months was documented in 31% of patients treated with pomalidomide with low-dose dexamethasone (LoDEX) in RRMM patients[47]. Lastly, selinexor plus dexamethasone resulted in objective treatment responses in patients with myeloma refractory to currently available therapies and a PR or better was observed in 26% of patients[47]. Our results suggest that vactosertib leads to clinical improvement with potential long-term benefits for patients in whom other available therapies have not been effective.

Since elevated TGFβ levels in patient sera are a hallmark of drug resistance in MM, vactosertib and pomalidomide are of clinical interest[48]. While increased TGFβ is associated with higher ISS stage and greater disease burden, to our knowledge, TGFβ has not been directly linked to the cytogenetic events that have been associated with high-risk myeloma[49,50]. Characterizing TGFβ levels in high-risk patients represents an important future direction that may inform clinical trial enrollment.

The frequency and severity of AEs were equal to or less than those observed with other regimens for RRMM. The most common toxicities and AEs, e.g., fatigue, cough, and pain, were infrequent, reversible and manageable. Clinically significant bleeding, respiratory, cardiac and infectious events were uncommon and non-hematological toxicities were infrequent. Permanent treatment discontinuation was very low. The proportion of secondary malignancies reported was zero, despite the inclusion of a significant number of patients with a longstanding history of MM and IMiD and alkylator exposure. Second primary malignancy in prior first-line, phase 3 studies has ranged from 2.5 to 10.7%, due to underlying disease and treatment-related effects[51].

https://doi.org/10.1038/s41467-024-51442-2

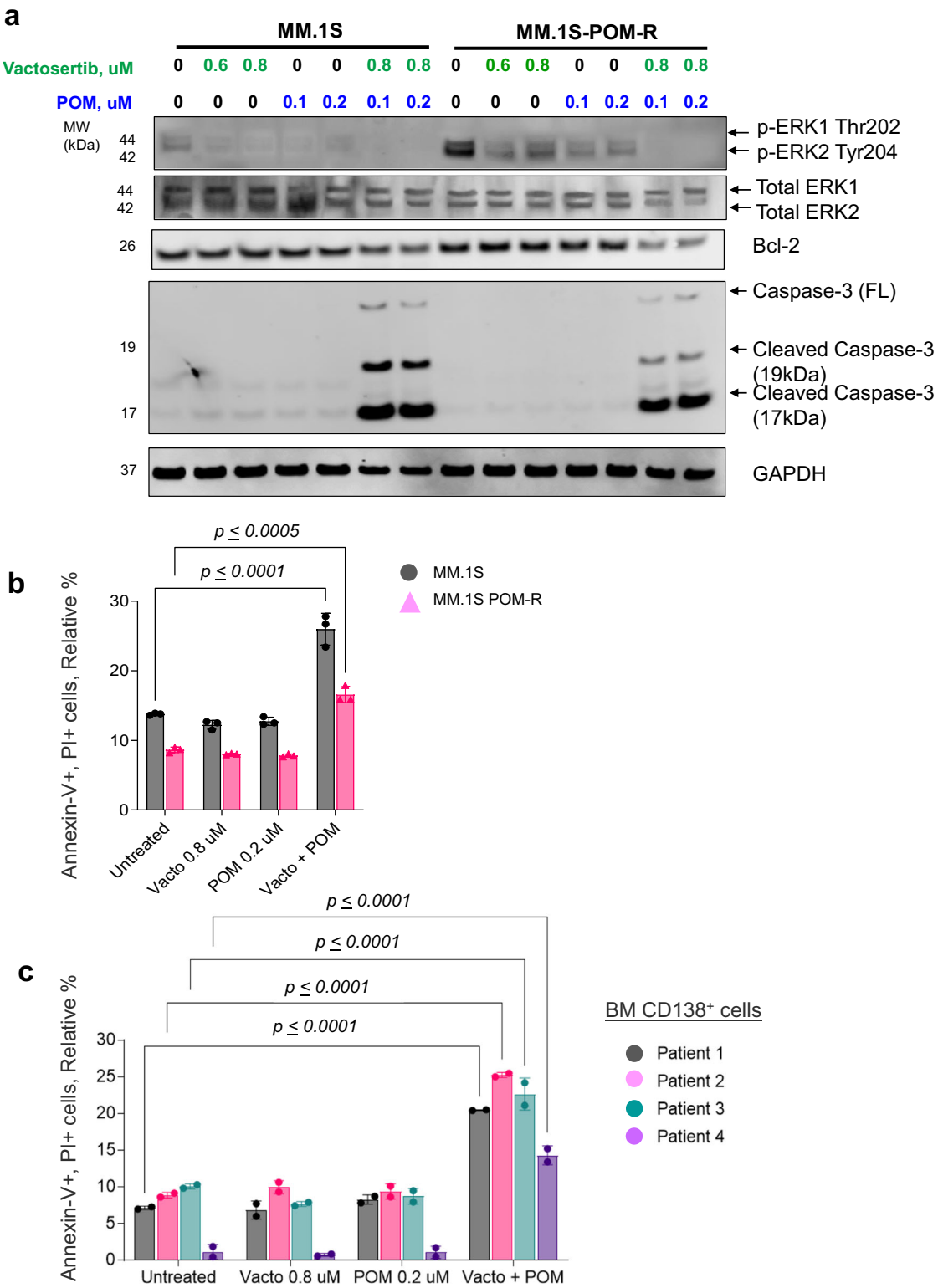


**Fig. 4 | Synergistic effect of vactosertib and pomalidomide on apoptosis in MM cells. a** Western blot analysis of MM1.S parental and pomalidomide-resistant cells treated with vactosertib and pomalidomide alone or in combination. Cells were treated with drugs as indicated, lysates prepared and probed with antibodies to phospho-ERK1/2, total ERK1/2, Bcl-2 and full-length (FL), cleaved caspase-3 and GADPH. Experiments were independently performed twice. **b** Combined effect of vactosertib and pomalidomide on MM1.S and MM1.S- pomalidomide-resistant cells. Cells ($1 \times 10^6$/assay) were incubated with drugs for 20 h, washed with PBS, lysates prepared, probed using antibodies specific to annexin-V (BD Biosciences, 556419) and propidium iodide (PI) (Invitrogen, P21493) and analyzed by flow cytometry (Attune NxT). Relative % of annexin-V+/PI+ cells represents the percent of drug treated MM cells relative to untreated cells. **c** Combined effect of vactosertib and pomalidomide on patient BM CD138$^+$ cells. Cells (~$1 \times 10^5$/assay) were incubated with drugs for 20 h, washed with PBS, probed using antibodies specific to annexin-V (BD Biosciences, 556419) and PI and analyzed by flow cytometry. Annexin-V+/PI+ cells represent the percent of CD138$^+$ cells positive for both annexin-V and PI relative to untreated cells. In (**b**) and (**c**), data are representative of three independent experiments. Error bars represent the SD of the mean (SEM). Two-way ANOVA was conducted to investigate potential interactions between more than two variables in (**b**) and (**c**).

https://doi.org/10.1038/s41467-024-51442-2

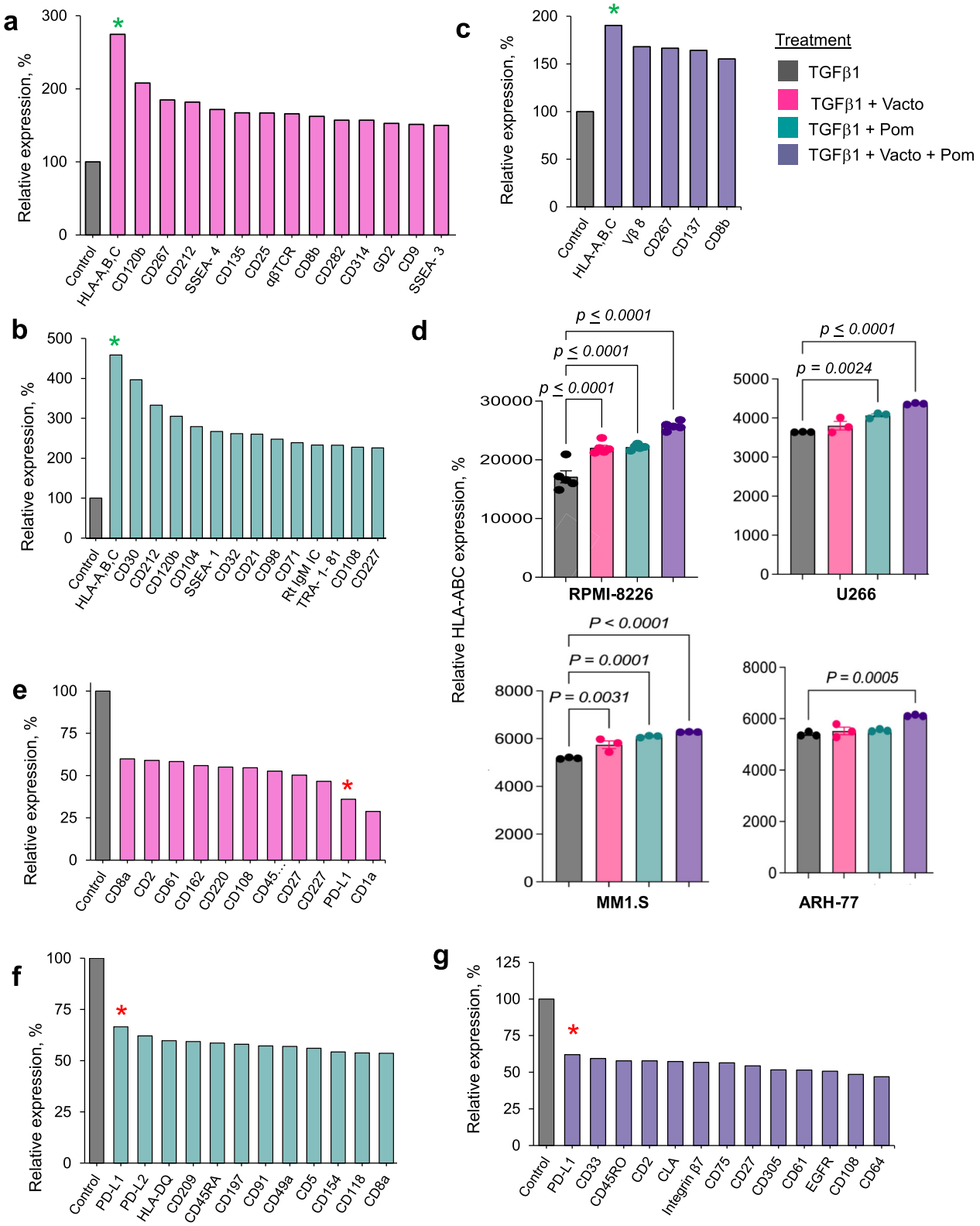


Biopsy from the single grade 4 hepatotoxicity showed pathologic findings suggestive of drug-induced hepatocellular injury with a non-specific pattern. Sporadic cases of severe hepatotoxicity have been reported for thalidomide, lenalidomide and pomalidomide[52]. Previously, it was noted that IMiDs may cause mild transaminitis in 1–2% of patients. A recent case report indicated that the level of severe acute liver injury is associated with either cholestatic or hepatocellular patterns of injury[53]. Major hepatotoxicity for the FDA-approved agent luspatercept, a TGFβ receptor/activin ligand trap used in clinical practice for low-grade MDS, has not been reported[54]. TGFβ plays an important role in the response to acute liver injury and conceivably could potentiate pomalidomide-related injury[53]. The true toxicity rate of this combination, and hepatotoxicity specifically, will be carefully monitored in phase II trials.

https://doi.org/10.1038/s41467-024-51442-2

**Fig. 5 | Effect of TGFβ1, vactosertib and pomalidomide on myeloma immunophenotype.** High-throughput cell surface marker screening to determine the effect of vactosertib, pomalidomide and TGFβ1 on MM surface antigens using the human cell surface marker screening panel (BD Biosciences, #560747). The screening panel contained 242 purified monoclonal antibodies to detect individual human cell surface markers. RPMI-8226 cells were treated with either TGFβ1 (10 ng/mL), TGFβ1 + vactosertib (1 μM), TGFβ1 + pomalidomide (1 μM), or TGFβ1, vactosertib and pomalidomide for 48 h. Following treatment, cells were washed and probed with the antibody array panel for 30 min. Cells were probed with Alexa Fluor 647-conjugated goat anti-mouse Ig or goat anti-rat Ig secondary antibodies. Isotype controls were included to determine the isotype-specific background. Cells were analyzed using a high-throughput flow cytometry (BD LSR Fortessa). Shown are surface markers: **a** increased by vactosertib + TGFβ1, **b** increased by pomalidomide + TGFβ1 and **c** increased by vactosertib, pomalidomide, and TGFβ1. Green asterisks (*) in (**a**–**c**) measure the effect of vactosertib, pomalidomide and both combined on the expression of HLA-ABC on RPMI-8226 cells. **d** Indicates the effect of TGFβ1 alone (grey), TGFβ1 + vactosertib (pink), TGFβ1 + pomalidomide (green) and TGFβ1 + vactosertib + pomalidomide (blue). In panel (**e**) are shown surface markers decreased by treatment with TGFβ1 and vactosertib, **f** surface markers decreased by treatment with TGFβ1 and pomalidomide and **g** surface markers decreased by treatment with TGFβ1, vactosertib and pomalidomide. Red asterisks (*) in (**e**–**g**) indicate the immunoinhibitory receptor PD-L1. Values in **a**–**c** and **e**–**g** were determined relative to the value measured for cells incubated with TGFβ alone (red bar). Following treatment and antibody staining, fluorescent intensity was measured by flow cytometry acquired using ≥10,000 events. Data were analyzed using FlowJo v10.8.1 software (Ashland, OR). Baseline values for isotype controls were subtracted from each reading. Values in (**d**) represent the average of five replicates for RPMI-8226 cells and three replicates for other cell lines. Source data are provided as a Source Data file.

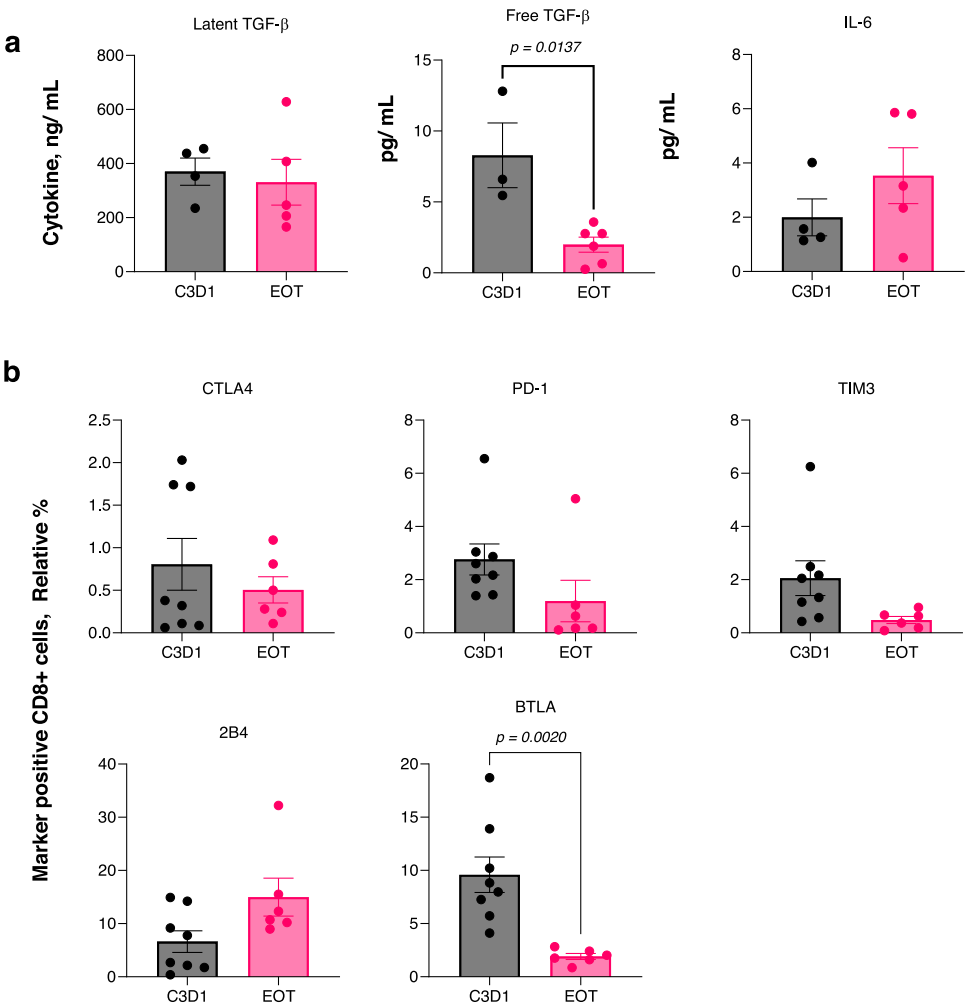


**Fig. 6 | Effect of vactosertib and pomalidomide in vivo treatment on patient BM cytokine and cellular components. a** Effect of vactosertib and pomalidomide on cytokine levels in patient BM samples. At the indicated times, latent TGFβ1, free (active) TGFβ1 and IL-6 levels were measured in patient BM samples ($n = 8$ samples at C3D1 and 6 samples at EOT). **b** Effect on vactosertib and pomalidomide on relative surface expression of the immunosuppressive markers PD-1, TIM-3, 2B4, BTLA and CTLA-4 on patient $CD8^+$ T-cells present within the BMMC fraction. The percent of PD-1, TIM-3, 2B4, BTLA and CTLA-4-positive staining cells were quantitated at indicated times. The relative percent of marker-positive cells was determined compared to cells obtained at C3D1. Data represent three independent experiments. In (**a**, **b**), differences between two groups were analyzed using the unpaired *T*-test. Error bars represent the SD of the mean (SEM).

While corticosteroids have historically been the backbone of most myeloma-targeting therapies, their efficacy must be balanced with a considerable side-effect profile of acute and chronic toxicities[12,55–57]. Steroids impair T-lymphocyte activation, reduce helper T-cell expansion, block regulatory T-cell recruitment and promote M2 macrophage polarization. The presence of concomitant disease that requires high-dose corticosteroids represents exclusion criteria for immunotherapy trials. Dexamethasone, a key agent in myeloma induction regimens, is associated with side effects that disproportionately affect older patients. Newer agents with significant anti-myeloma activity now permit the development of steroid-free regimens. Despite the absence of steroids, the time to response did not appear significantly delayed with vactosertib since the median time to a first response was 1–2 months and the median time for best response was 2 months. This

https://doi.org/10.1038/s41467-024-51442-2

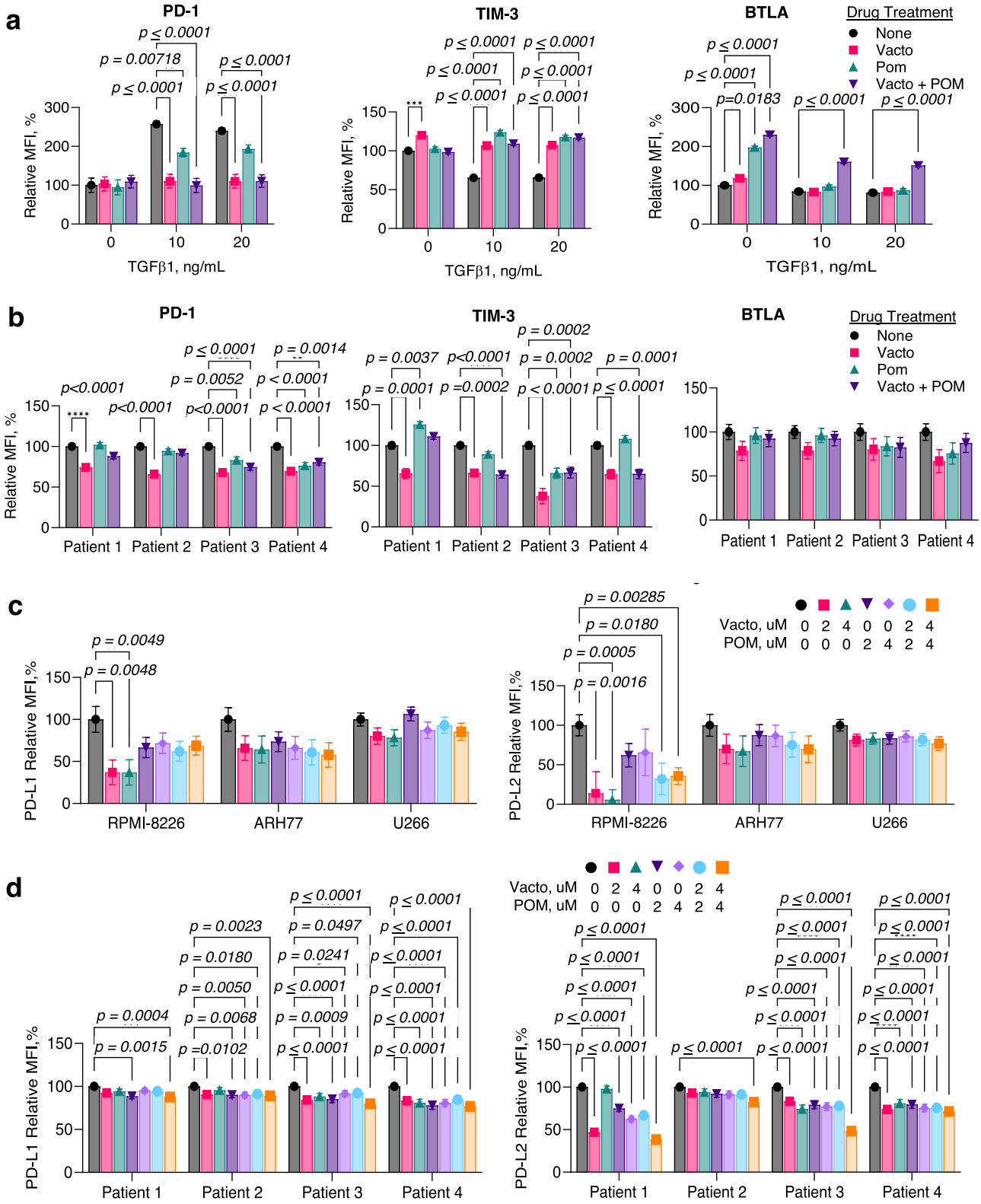


**Fig. 7 | Direct effect of vactosertib to CD8⁺ T-cell immunophenotype. a** Shown is the relative MFI value for the expression of each immunosuppressive marker (PD-1, TIM-3, BTLA, and LAG-3) on CD8⁺ T-cells isolated from healthy peripheral blood. T-cells were cultured in the presence of TGFβ1 at indicated concentrations. CTLA-4 was not detected by immunostaining of healthy human T-cells. Error bars represent the SD of the mean. **b** Shown are relative MFI values after staining for PD-1, TIM-3 and BTLA on MM patient CD8⁺ T-cells. Error bars represent the SD of the mean. **c** Effect of vactosertib on PD-L1 and PD-L2 expression on MMCLs. MMCLs were treated with vactosertib and pomalidomide as indicated for 72 h. Cells were then stained with PD-L1 and PD-L2 antibodies for 20 min and analyzed by flow cytometry. **d** Effect of vactosertib on PD-L1 and PD-L2 expression on MM patient BM-derived CD138⁺ cells. Patient CD138⁺ cells were treated with vactosertib and/or pomalidomide at various concentrations for 48 h. Cells were then stained with PD-L1 and PD-L2 specific antibodies simultaneously for 20 min and analyzed by flow cytometry. Statistical comparisons were made by comparing drug treated to untreated cells. In (**a**–**d**), values represent the average of triplicate measurements. Two-way ANOVA was conducted to investigate potential interactions between more than two variables in (**a**–**d**). Source data are provided as a Source Data file.

https://doi.org/10.1038/s41467-024-51442-2

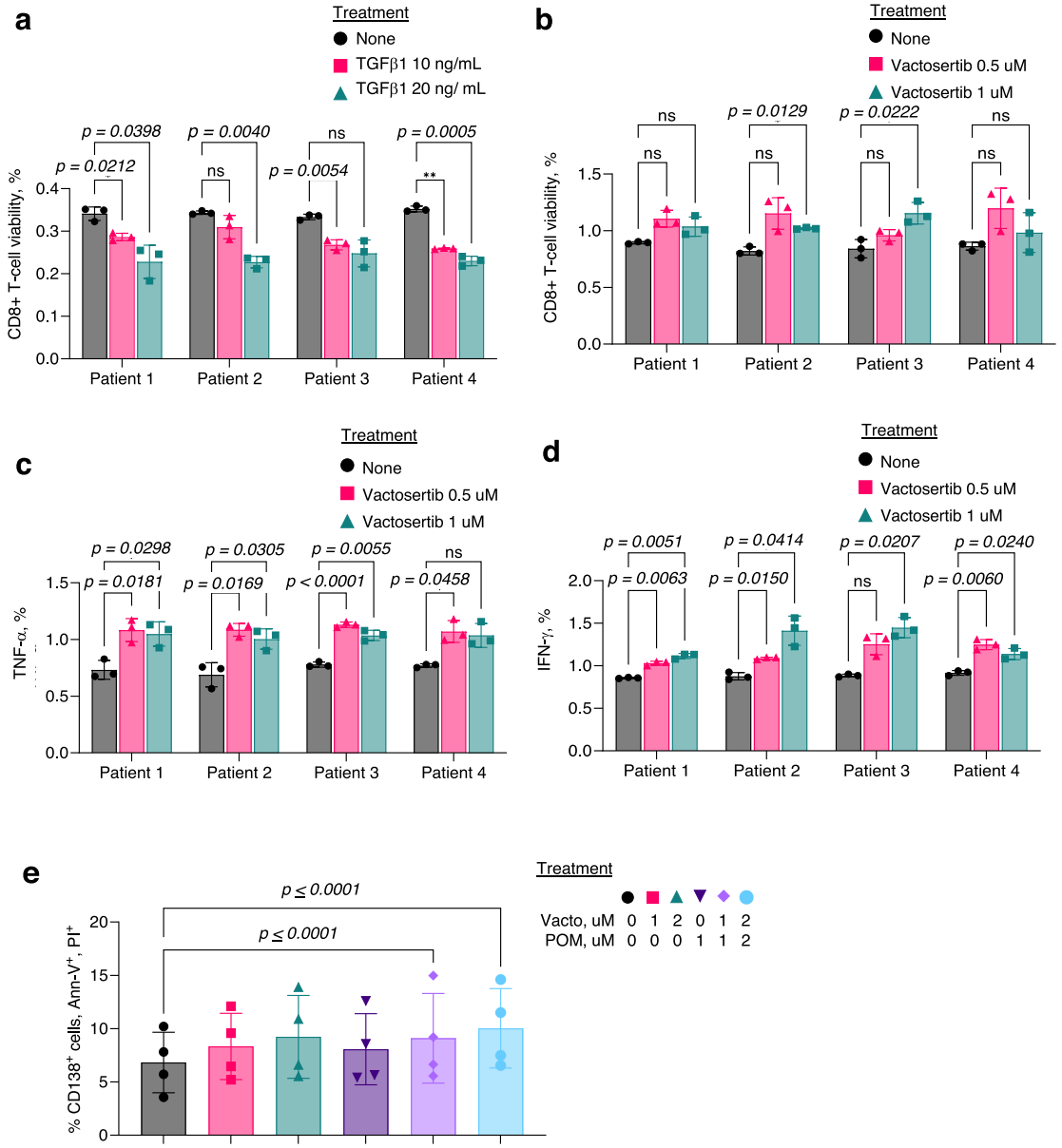


**Fig. 8 | Direct effect of vactosertib on CD8⁺ T-cell cytolytic activity. a** Effect of TGFβ1 on the viability of patient CD8⁺ T-cells. Cells (5000/well) were treated as indicated for 24 h. Activated-XTT assay solution was added and plates were incubated in the dark for 3 h. Relative cell viability was quantified by measuring the absorbance at 450 nm on a SpectraMax i3x multi-mode microplate reader. **b** Effect of vactosertib on the viability of patient CD8⁺ T-cells in the presence of TGFβ1. Cells (5000/well) were treated as indicated for 24 h. Activated-XTT assay solution was added and plates were incubated in the dark for 3 h. Relative cell viability was quantified by measuring the absorbance at 450 nm on a SpectraMax i3x multi-mode microplate reader. **c** Effect of vactosertib on TNF-α production by MM patient CD8⁺ T-cells. Cells (5000/well) were incubated with vactosertib at indicated concentrations for 24 h. Culture supernatant was centrifuged at 1000 × *g* for 5 min and cytokine level quantitated using the human TNF-α Quantikine ELISA kit. **d** Effect of vactosertib on IFN-γ production by patient CD8⁺ T-cells. Cells (5000/well) were incubated with vactosertib at indicated concentrations for 24 h. Culture supernatants were centrifuged at 3000 rpm × 5 min. Cytokine levels were quantitated using the human IFN-γ Quantikine duoSet ELISA kit. **e** Effect of vactosertib on autologous CD8⁺ T-cell cytotoxic activity. Shown is the effect of vactosertib and pomalidomide on autologous CD8⁺ T-cell activity against patient CD138⁺ cells. CD138⁺ cells (20,000/well) were treated as indicated for 8 h and then co-cultured with CD8⁺ T-cells (50,000/well) for 18 h. Cells were then stained to detect CD138⁺ cells followed by annexin-V and PI staining. Cells that gated positively for CD138⁺, annexin-V and PI were quantitated by flow cytometry using FlowJo_10.8.1 software. In (**a**–**e**), values represent the average of triplicate measurements ($n = 3$). Two-way ANOVA was conducted to investigate potential interactions between more than two variables (**a**–**e**). In panel (**a**), two asterisks (**) indicate a *p*-value ≤ 0.01. Source data are provided.

compares favorably with previously reported steroid-containing regimens, e.g., bortezomib and thalidomide with or without dexamethasone, with a median time to response of ~1.4–2 months[58,59]. The efficacy and favorable safety profile of vactosertib administered in steroid-sparing regimens may improve the treatment of elderly patients at greater risk of treatment toxicity and poor survival due to their age and comorbidities.

Our results, and prior studies, suggest a complex paradigm of TGFβ signaling wherein SMAD2/3 interact with other signaling cascades, including the ERK/MAP kinase pathway[60,61]. Whereas the TGFβRI transduces the signal through its serine/threonine kinase activity, the ERK/MAP kinase pathways have been attributed mainly to either growth factor stimulation of RTKs or activation by stress-related stimuli. Prior evidence has shown that TGFβ activates the ERK/MAP

kinase pathways in certain cancer cell lines. Thus, although these pathways were initially described as being isolated and linear, it has become increasingly apparent that they are mutually regulated through interaction(s) at multiple levels. Interaction with the ERK pathway seems to be cell type- and target gene-specific, as it has been variably reported to enhance or inhibit SMAD activity. IMiDs have markedly improved patient outcome in MM, however, IMiD resistance commonly underlies relapse. IMiDs trigger additive or synergistic anti-MM activity when combined with proteasome inhibitors and monoclonal Abs in preclinical models and are now used in combinations to treat both newly diagnosed and relapsed MM. Activation of nuclear factor κB and Raf–mitogen-activated protein kinase-MEK-–ERK promoting migration, proliferation, survival and drug resistance. Prior studies have demonstrated that MEK inhibitor combination treatment restored IMiD sensitivity to MM cells in vitro and in vivo. Vactosertib represents a safe and efficacy approach to restore IMiD sensitivity and provides the framework for clinical trials to overcome IMiD resistance and improve patient outcome in MM.

T-cell fitness is predicted to limit $CD8^+$ T-cell cytolytic activity and T-cell function and phenotype. Inhibitory effects of TGFβ on $CD8^+$ T-cell function were previously indicated in vivo by studies showing that interfering with TGFβ signaling either by T-cell-specific TGF dominant negative receptor (TGF-DNRII) expression or by administration of a soluble TGFβRII, led to enhanced immune responses against transplantable tumors[62]. The observation that TGFβ acts directly upon $CD8^+$ T-cells to control their differentiation was definitively established by the finding that TGF-βRII-deficient $CD8^+$ T-cells produce increased amounts of IFN-γ and other cytolytic molecules. Gorelik and Flavell demonstrated that T-cell-specific blockade of TGFβ signaling allows for the generation of an immune response capable of eradicating tumors in mice challenged with live tumor cells[63,64]. The results suggest that in the absence of TGFβ signaling, T-cells are able to mount a potent tumor-specific CTL response that promotes tumor regression. As a negative regulator of anti-tumor immunity, TGFβ1 impairs the efficacy of anti-PD-1/PD-L1 directed therapy and promotes drug resistance. PD-1 expression on T-cells serves as an immune checkpoint to attenuate downstream T-cell receptor (TCR) signaling and limit T-cell activation, while TGFβ1 directly inhibits effector T-cells[65,66]. Therapeutic antibodies that target the PD-1/PD-L1 axis induce potent and durable anti-tumor responses in multiple cancer types but only in limited patient populations[67]. Our studies to characterize molecular mechanisms that govern T-cell-mediated treatment responses demonstrate that TGFβ1 promotes that vactosertib suppresses the TGFβ1-driven upregulation of PD-1 (Fig. 9). Vactosertib also reduced PD-L1/PD-L2 on MM cells and enhanced T-cell activity. Vactosertib may also modulate the MHC class I antigen presentation machinery since we observed an increase in expression of the pan-HLA-ABC molecule on $CD138^+$ cell surface in response to vactosertib. Our analysis is consistent with prior studies that showed that exhausted T-cells are enriched within the TME but possess immunophenotypic and functional plasticity[68]. Neoadjuvant immunotherapy to target immunosuppression offers advantages over upfront surgery and adjuvant therapy, including the potential to improve clinical outcomes and understand molecular mechanisms of treatment response and resistance. Vactosertib may serve an immune adjuvant and neoadjuvant role to block TGFβ1 signaling and revert the exhausted T-cell phenotype that precludes responses in RRMM and solid tumors.

Grenga et al. studied the first-in-class bifunctional fusion protein M7824 comprised of a monoclonal antibody against PD-L1 fused to the extracellular domain of the human TGFβ receptor 2, which functions as a TGFβ trap[67]. The rationale for a combined molecule is to block the PD-1/PD-L1 interaction between tumor cells and immune cell infiltrate and simultaneously reduce or eliminate TGFβ from the TME. In contrast to PD-L1 inhibition alone, dual blockade of PD-L1 and TGFβ, using a novel bifunctional fusion protein, modulated human urothelial cancer cell phenotype, rendering cells more susceptible to TRAIL and antigen-specific $CD8^+$ T-cell mediated lysis. Dodagatta et al. showed that α-PD-1 not only initiates a tumor rejection program, but can induce a competing TGFβ-driven immunosuppressive program. An α-TGFβ antibody was also shown to suppress immunosuppressive Tregs induced by α-PD-1, which limit the anti-tumor activity of α-PD-1 monotherapy[69].

Recent studies have harnessed the power of T-cells engineered to express CARs to treat MM and other hematologic malignancies[70–72]. Barriers to effective CAR T-cell therapy include severe life-threatening toxicities, modest anti-tumor activity, antigen escape, restricted trafficking and limited tumor infiltration. Furthermore, host and TME interactions critically alter CAR T-cell function, while a complex workforce is required to develop, expand and implement these treatments. Strategies to block TGFβ1 signaling and improve the next generation of armored CAR T-cells, TCRs and BiTEs are rapidly advancing for clinical evaluation[73].

## Methods

### Study design and participants

In this single-center, single-arm, phase 1b study, we enrolled patients aged ≥18 years from the Seidman Cancer Center (Cleveland, OH, USA) who had a diagnosis of RRMM, measurable disease and adequate organ function. Patients had received ≥2 previous lines of therapy including IMiD and proteasome inhibitor. Patients were eligible if they were refractory to their last line of therapy and had an ECOG performance status of ≤2. Between July 1, 2017 and June 30, 2022, patients were enrolled on the IRB-approved protocol following good practice guidance and protected under the Helsinki Declaration (see Supplementary Information for full protocol). The protocol underwent two key amendments to optimize treatment strategies. The first amendment on 4/19/2019 adjusted the frequency of vactosertib administration from daily to twice daily for patients enrolled on the third dose level and beyond. The modification was prompted by emerging data from concurrent trials of vactosertib[30]. Second, on 3/31/2020, the duration of therapy was extended to 12 months. This decision stemmed from promising findings of excellent tolerability and high progression-free survival (PFS) observed at the 6-month mark during the 3 + 3 phase. These amendments aimed to refine the protocol and to maximize potential patient outcome based on evolving clinical insights.

A total of 22 patients were evaluated for trial enrollment. Patient #14 was deemed ineligible. Patient #16 self-withdrew prior to receiving any study drug. Pt. #20 developed grade 4 hepatotoxicity during cycle 2 of treatment. While this AE led to the patient's withdrawal from the study, since the patient had received vactosertib treatment, he was included in the primary analysis population. Therefore, all patients exclusive of #14 and #16, were included in the analysis of patient demographics, treatment efficacy, best response, drug toxicity, AEs, severe AEs, DLTs, PK and translational studies. Evaluation of drug safety considered AEs, severe AEs, DLTs, physical examinations, vital signs and clinical laboratory values, as potential reasons for treatment discontinuation. Participants received vactosertib in combination with pomalidomide in the trial performed in a classical 3 + 3 dose escalation phase I study with an extension cohort. During each 28-day treatment cycle, vactosertib was administered for 5 consecutive days weekly for 4 weeks (days 1–5, 8–12, 15–19, 22–26) with a 2 day rest period included each week (days 6–7, 13–14, 20–21 and 27–28) (Fig. 1a). Vactosertib was given at dose levels of 60 mg qd, 120 mg qd, 100 bid and 200 mg bid per the treatment schedule. Pomalidomide was administered at 4 mg po qd for 21 consecutive days at the initiation of each 28-day cycle. Primary endpoints were the safety and tolerability profile of vactosertib and pomalidomide and to determine the MTD. Primary analysis was done per protocol, in the all-treated and efficacy-evaluable population. Secondary endpoints were CBR [defined as the summation of patients that exhibited a complete response (CR), very good

https://doi.org/10.1038/s41467-024-51442-2

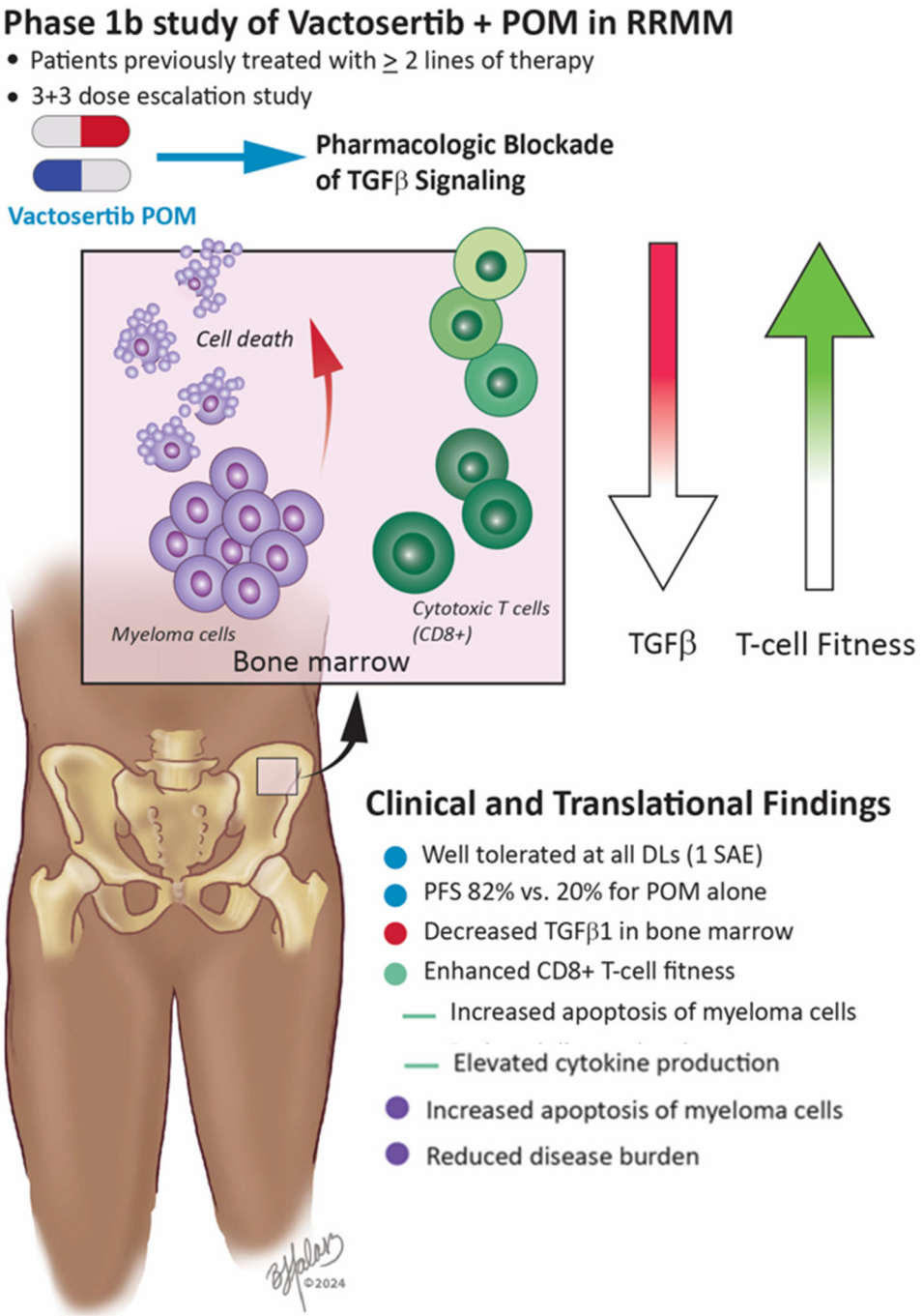


**Fig. 9 | The TGFβ type I receptor kinase inhibitor vactosertib in RRMM: a phase 1b trial.** Relapsed and/or refractory multiple myeloma patients previously treated with ≥2 lines of therapy were enrolled on a phase 1b study to assess safety and recommend a phase two dose of vactosertib in combination with the immunomodulatory drug pomalidomide. Shown are the putative combined in vivo effects of vactosertib and pomalidomide therapy in RRMM patients.

partial response (VGPR), PR, MR, or SD] based on IMWG criteria, response duration, PK and PF. The effect of vactosertib and pomalidomide on TGFβ1 and IL-6 levels, $CD138^+$, $CD38^+$ cells, $CD4^+$ $CD8^+$, NK cells, macrophages, monocytes and myeloid-derived suppressor cells from patient BM was measured. The study is registered with ClinicalTrials.gov., NCT03143985, completed and survival follow-up is ongoing.

### Ethics approval and consent to participate

The study was approved by the Institutional Review Board (IRB) at University Hospitals, Cleveland Medical Center, Cleveland, OH. The study is registered with ClinicalTrials.gov., NCT03143985. Informed consent was obtained for trial participation and to obtain BM and blood samples from patients and healthy donors.

### Inclusion and exclusion criteria

All inclusion and exclusion criteria are listed in the IRB-approved protocol (see Supplementary Information).

### Procedures

All patients received pomalidomide orally on days 1–21 of a 28-day cycle as indicated in the treatment cycle, until progression or intolerance, for up to 24 months on protocol. Thromboprophylaxis was required at a minimum of 81 mg of aspirin. Response assessments were

made using laboratory tests specified by the IMWG Uniform Response Criteria on clinic visits on day 1 of indicated cycles and on day 1 of every third cycle starting with cycle 2. Patients had BM aspirates and biopsy samples taken at baseline and at progression or end of the study. Patients were removed from the study if they had disease progression, withdrew consent, had a diagnosis of new malignancy requiring systemic therapy, or developed unacceptable toxic effects. AEs were monitored during clinic visits, hospitalizations, and via documented patient-initiated phone conversations, and categorized per the National Cancer Institute (NCI) Common Terminology Criteria for Adverse Events (CTACE, version 4.0). AEs were considered serious if they resulted in death, were life-threatening, required unplanned hospitalization, or resulted in persistent or significant incapacity or disruption of ability to conduct normal life functions. Intra-patient dose modification, per protocol, was not performed for medication-related toxicity or AEs.

### Outcomes

The primary endpoint was the safety of vactosertib combined with pomalidomide as defined by CTACE criteria as the time of enrollment until disease progression, serious AE or death. Drug safety considered the number of AEs, severe AEs, DLTs, as well as changes in physical examination, vital sign, and clinical laboratory value. Secondary endpoints were to determine the effect of vactosertib and pomalidomide on PFS at 6 months (PFS-6), response rates, PK properties and effects of vactosertib on patient cytokines, tumor cells and immune cells. PFS-6 was determined as in the multicenter, randomized phase 2 study assessed the efficacy and safety of pomalidomide with/without LoDEX in patients with RRMM[29].

### Statistical analysis of outcome

PFS at 6 months and event-free survival were estimated using the Kaplan–Meier method. We estimated associations of PFS with a univariate Cox proportional hazards model. Analyses were performed using RStudio version 1.2.5.

### Patient samples

Patient samples were obtained and de-identified following IRB approval and informed consent. Peripheral blood samples were barcoded and stored at −80 °C. BM samples were processed to isolate the mononuclear cell fraction by red blood cell lysis following by gradient centrifugation. $CD138^+$ cells were isolated by positive selection using the EasySep™ human CD138 positive selection kit II (StemCell Technology, Cambridge, MA). $CD8^+$ T-cells were isolated using the EasySep direct human $CD8^+$ T-cell isolation kit (StemCell Technology).

### Cell lines

Authenticated MMCLs RPMI-8226, ARH77, U266, MM1.S, MM1.R and NCI-H929 were obtained from ATCC (Manassas, VA) and cultured under standard conditions in complete RPMI media that contained pen/strep and glutamine. Cell lines were tested for mycoplasma using the Mycostrip detection kit and biobanked for future use. Cultures were replaced regularly from frozen stock. High cell density cultures were split 1:2 every 3 days.

### Chemicals

Vactosertib, pomalidomide and lenalidomide were from Selleck Chemicals (Houston, TX). DMSO, XTT tetrazolium salt (sodium 3′-[1-[(phenylamino)-carbony]-3,4-tetrazolium]-bis(4-methoxy-6-nitro)benzene-sulfonic acid hydrate), PMS (*N*-methyl dibenzopyrazine methyl sulfate) and general chemicals were from Sigma Chemical Co. (St. Louis, MO).

### Antibodies

To quantitate the relative level of individual cell types, patient BM-derived mononuclear cell fractions were stained with the following antibodies: FITC-conjugated anti-human CD19 antibody (Biolegend: 302205), PE/Cyanine7-conjugated anti-human CD8 antibody (Biolegend: 344711), FITC-conjugated anti-human CD38 antibody (Biolegend: 303504), PerCP/Cyanine5.5-conjugated anti-human CD138 (Syndecan-1) antibody (Biolegend: 356509), Pacific Blue™-conjugated anti-human CD45 antibody (Biolegend: 368540), APC-conjugated anti-human CD14 antibody (Biolegend: 367118), APC-conjugated anti-human CD16 antibody (Biolegend: 302012), APC-conjugated anti-human CD3 antibody (Biolegend: 317318), FITC-conjugated anti-human CD56 (NCAM) antibody (Biolegend: 318303), PE-conjugated anti-human CD80 antibody (Biolegend: 305207) to detect M1 MACS and FITC-conjugated anti-human CD163 antibody to detect M2 MACS. To quantitate the relative expression of immunosuppressive surface markers on $CD8^+$ T-cells, cells were stained with antibodies specific to PD-1 (Biolegend: 329952), TIM-3 (Biolegend: 364806), LAG-3 (Biolegend: 369343), BTLA (Biolegend: 344524) and CTLA-4 (Biolegend: 369606) according to manufacturer's guidelines. PE/Cyanine7-conjugated anti-human CD138 (Syndecan-1) antibody (Invitrogen: 25-1389-41) was used to stain patient myeloma cells. Human normal peripheral blood $CD8^+$ Cytotoxic T-cells (HumanCells Biosciences, Milpitas, CA: PBCD-C10M) were treated with recombinant human TGFβ1 (HEK293-derived, Peprotech: 100-21) at 0, 5, 10, 20 and 30 ng/mL for 48 h and probed with antibodies specific for CTLA-4, PD-1, BTLA, TIM-3 and LAG-3. To quantitate relative PD-L1 and PD-L2 expression, cells were stained with FITC-conjugated anti-human CD274 (B7-H1, PD-L1) (Biolegend: 393606) and APC-conjugated anti-human CD273 (B7-DC, PD-L2) (Biolegend #345508) according to the manufacturer's guidelines.

### Cell viability

Cell viability was measured using the XTT assay[74]. Cells were added to 96-well plates in RPMI media that lacked phenol red. Drugs were added at indicated concentrations and plates were incubated under standard conditions. Activated-XTT reagent was then added, plates were incubated at 37 °C and absorbance measured at 450 nm.

### Isolation of MM patient BM $CD138^+$ and $CD8^+$ T-cells

BM samples were obtained from patients at indicated times and BMMC cells were isolated after RBC lysis and density centrifugation. $CD138^+$ cells were isolated from the BMMC fraction using the EasySep™ human CD138 positive selection kit II (StemCell Technology, Cambridge, MA). $CD8^+$ T-cells were isolated from the BMMC fraction using the EasySep direct human $CD8^+$ T-cell isolation kit (StemCell Technology). T-cells were enriched from the BMMC fraction.

### Flow cytometry

Healthy human T-cells (HumanCells Biosciences, Milpitas, CA) and MM patient T-cells and $CD138^+$ cells were washed, resuspended in 100µL FACS staining buffer with markers and respective isotype controls at room temperature followed by three washes. Samples were analyzed using an Attune NxT flow cytometer (ThermoFisher Scientific, Waltham, MA). Data were acquired and analyzed using FlowJo v10.8.1 software (Ashland, OR).

### Western blots

MM1.S cells were treated at a density of $1 \times 10^6$ cells/mL with 1 µM pomalidomide for 18 h with or without 10 ng/mL TGFβ1 for 60 min. Lysates were prepared using RIPA buffer (Invitrogen, 89901) with protease and phosphatase inhibitors (Cell Signaling Technology (CST), 5872) according to the manufacturer's protocol. Equal amounts of proteins were subjected to SDS–PAGE followed by transfer to PVDF membranes. Membranes were probed using the following antibodies: CBRN (CST, 71810), IKZF1/Ikaros (CST, 14859), IKZF2/Helios (CST, 89270), IKZF3/Ailos (CST, 15103), IKZF4 (Abcam, ab170957), IKZF5 (Invitrogen, PA5-110798), IRF4 (CST, 62834), Phospho-SMAD2 (Ser465/467)/SMAD3 (Ser423/425) (CST, 8828), total SMAD2/3 (CST, 8685),

phospho-p44/42 MAPK (ERK1/2) (Thr202/Tyr204) (CST, 4370), p44/42 MAPK (ERK1/2) (CST, 9102), phospho-Akt (Ser473) (CST, 4060), total-Akt (CST, 9272), c-Myc (CST, 18583), phospho-c-Myc (Thr58) (CST, 46650), phospho-c-Myc (Ser62) (CST, 13748), TRAF2 (CST, 4724), phospho-Stat3 (Tyr705) (CST, 9145), cleaved caspase-3 (CST, 9661), Bcl-2 (CST, 15071) and GAPDH (CST, 97166). Samples were loaded on 4–12% precast 1 mm bis–tris gels (Biorad, Hercules, CA) and electrophoresed for 4 h at 180 V. Proteins were transferred to PVDF membranes (Millipore, Bedford, MA) for 4 h at 4 °C and stained with primary antibodies diluted 1:2000. Membranes were stained with LiCor secondary antibodies at 1:2000 (LI-COR Biosciences Cat #926-68023, RRID:AB_10706167). Secondary antibodies were IR dye 680LT donkey anti-rabbit (red) 926-68023, IR dye 800 CW donkey anti-rabbit (green) 926-32213, and IR dye 800 CW goat anti-mouse (green) (LI-COR Biosciences, Littleton, CO, Cat #926-32210 RRID:AB621842). Membranes were imaged using a Li-COR system interfaced with the Odyssey-CLx and Imaging Studio 4.0 software.

### Generation of a pomalidomide-resistant MM1.S cell line

MM1.S cells resistant to pomalidomide were generated by culturing parental MM1.S cells in the presence of pomalidomide for >10 weeks. Briefly, MM1.S cells were cultured in a complete medium that contained pomalidomide at 50 nM and increased gradually until concentrations exceeded 2.5 μM.

### MM cell surface marker analysis

The BD Lyoplate™ human cell surface marker screening panel contained 242 purified monoclonal antibodies directed against cell surface markers (BD Biosciences, Heidelberg, Germany). The panel also contained both mouse and rat isotype controls to assess isotype-specific background. The BD Lyoplate screening panel was used to characterize the effect of TGFβ1, vactosertib and pomalidomide on the expression of surface markers on RPMI-8226 cells and was performed according to the manufacturer's instructions. Plates that contained the lyophilized antibodies were centrifuged at 300 × *g* for 5 min and then reconstituted in 110 μL of sterile PBS. RPMI-8226 cells were harvested, washed in PBS and resuspended in Pharmingen stain buffer containing 5 mM EDTA at a concentration of $1.25 \times 10^6$ cells/mL. Eighty microliters of cell suspension per well was then transferred to 96-well plates and stained with 20 μL of specific primary antibodies for 30 min on ice. Cells were washed twice with Pharmingen stain buffer containing 5 mM EDTA and stained with 100 μL of Alexa Fluor 647-labeled anti-mouse or anti-rat secondary antibody diluted 1: 200 for 30 min on ice. After washing, cells were fixed with BD cytofix fixation buffer and transferred from 96-well plates to single BD FACS tubes. Fluorescence was measured with a BD FACSCanto II cytometer using 10,000 cells/sample and FACSDiva software. Background fluorescence was set manually for each sample based on the appropriate isotype using FlowJo software. Results are expressed as the percentage of positive cells in the population and median fluorescence intensity (MFI).

### Cytokine assays

Cytokines were measured in freshly isolated patient BM samples and cell supernatants using the human latency-associated peptide (LAP) TGFβ1 Quantikine ELISA kit (R&D catalog # DLAP00), the human TGFβ1 duoSet ELISA kit (R&D catalog # DY240), the human IL-6 Quantikine QuicKit ELISA kit (R&D QK#206), the human IFN-γ duoSet ELISA (R&D catalog # DY285B) and the human TNF-α Quantikine ELISA kit (R&D catalog # DTA00D) from R&D systems (Minneapolis, MN) according to the manufacturer's instructions.

### Flow cytometry

Cells ($10^6$/100 μL) were stained with marker antibodies in FACS buffer (PBS, 1% BSA, 0.1% sodium azide) for 30 min at room temperature in the dark after which they were washed thrice before analysis using an Attune NxT Flow Cytometer. Unstained cells and isotype-specific controls were included with each assay.

### Annexin-V/propidium iodide staining

MM cells were incubated as indicated treatments or co-cultured with $CD8^+$ T-cells; where treatment mediated, or T-cell mediated cell death was evaluated by flow cytometry to detect annexin-V and PI-positive staining cells using the FITC Annexin V Apoptosis Detection Kit I (BD Biosciences, 556547).

### Assay method for measuring plasma concentration of vactosertib

Plasma concentrations of vactosertib were quantified by liquid-chromatography multiple reaction monitoring (LC-MRM). Stock solutions of vactosertib (MedChemExpress, Monmouth Junction, NJ) and internal standard (IS, valsartan, MedChemExpress) were prepared at 10 μg/mL in 0.1% formic acid. Serial dilution of vactosertib stock solution with 0.1% formic acid gave the corresponding working vactosertib solutions at concentrations of 390.625, 781.25, 1562.5, 3125, 6250, 12,500, 25,000, 50,000 and 100,000 ng/mL for preparation of calibration standards. The solutions were further diluted ten times with human plasma (Innovative Research, Novi, MI) and used as calibration standard samples. Plasma samples were thawed, and 10 μL of the IS stock solution was added to 10 μL of each sample. After a 10 s vortex, 80 μL of acetonitrile was added to each sample to precipitate proteins. The solution was then centrifuged at 14,000 × *g* for 10 min. The supernatant was transferred into a polypropylene insert (Agilent Technologies, Santa Clara, CA) and placed in a HPLC autosampler vial for LC-MRM analysis as described below. LC-MRM analysis was carried out using an Agilent 1290 Infinity HPLC system (Agilent, Santa Clara, CA) coupled with Agilent 6460 Triple Quadrupole mass spectrometer equipped with an electrospray Jet Stream ion source. Following the sample preparation described above, 1 μL of sample was injected onto a Kinetex 2.6 μm Polar C18 100 Å (100 × 2.1 mm) column (Phenomenex, Torrance, CA) and chromatographed using a linear gradient of acetonitrile from 20% to 80% over 8 min in aqueous 0.1% formic acid at a flow rate of 200 μL/min. Mass spectrometric analysis employed electrospray ionization in the positive ion mode with MRM at the transitions of m/z 400.1→289.1 for vactosertib and 436.1→291.1 for IS. The optimized fragmentor voltage and collision energy for vactosertib were 140 and 13 V, respectively, and 84 and 17 V for IS. The optimized ion source parameters were as follows: capillary voltage (2000 V), nozzle voltage (2000 V), nebulizer gas pressure (45 psi), sheath gas flow (11 L/min), and sheath gas temperature (300 °C). Nitrogen was used as the source and collision gas. Vactosertib and IS were eluted at 3.6 and 6.4 min, respectively. The developed LC-MRM method showed an excellent linearity between 39 and 5000 ng/mL with $r^2 > 0.99$. The acquired LC-MRM data were analyzed by Agilent MassHunter Quantitative Analysis software to determine the plasma concentrations of vactosertib. Log transformation was not made when analyzing the pharmacokinetic parameters of vactosertib. PK parameters were obtained from plasma concentration data using Ubiquity PK modeling tool[29].

### Quantification and statistical analysis methods

All bioassays were performed in triplicate unless noted otherwise. Population frequencies were exported from FlowJo and statistical significance was analyzed using Prism 8.4.1 software (GraphPad, Boston, MA) or Microsoft Excel (Redwood, WA). Summary plots were prepared using GraphPad Prism 10.1.0.316 (×64) or Microsoft Excel. In Fig. 6a, b, differences between two groups were analyzed using the unpaired *T*-test. Two-way ANOVA was conducted to investigate potential interactions between more than two variables (Figs. 4, 7, 8, S8, S9). *P* values were indicated as: ns—not significant and four asterisks (****) represent a $p$ value ≤ 0.0001. Error bars represent the relative SEM.

### Statistical analysis for the effect of vactosertib and pomalidomide on MMCLs and MM patient CD138$^+$ cells

Parental and pomalidomide-resistant MM1.S cells (Fig. 4b) and patient CD138$^+$ cells (Fig. 4c) were treated with vactosertib and pomalidomide. *Y*-axis represents the relative percent of annexin-V+/PI+ cells that were quantitated by flow cytometry. Raw data were analyzed by application of two-way ANOVA using Graphpad Prism Software.

### Reporting summary

Further information on research design is available in the Nature Portfolio Reporting Summary linked to this article.

## Data availability

The IRB-approved trial protocol is available in the Supplementary Information file. The statistical analysis plan and de-identified participant data will be made available upon request to the corresponding author. Data will be available for 1 year once access has been granted without restrictions on who the data can be made available to or for which purpose. The remaining data are available within the article, Supplementary Information or Source data file. Source data are provided with this paper.

## References


1. van de Donk, N. W. C. J., Pawlyn, C. & Yong, K. L. Multiple myeloma. *Lancet* **397**, 410–427 (2021).
2. Cowan, A. J. et al. Diagnosis and management of multiple myeloma: a review. *JAMA* **327**, 464–477 (2022).
3. Mateos, M. V., Nooka, A. K. & Larson, S. M. Moving toward a cure for myeloma. *Am. Soc. Clin. Oncol. Educ. Book* **42**, 1–12 (2022).
4. Pawlyn, C. & Morgan, G. J. Evolutionary biology of high-risk multiple myeloma. *Nat. Rev. Cancer* **17**, 543–556 (2017).
5. Kastritis, E., Terpos, E. & Dimopoulos, M. A. How I treat relapsed multiple myeloma. *Blood* **139**, 2904–2917 (2022).
6. Bazarbachi, A. H., Al Hamed, R., Malard, F., Harousseau, J. L. & Mohty, M. Relapsed refractory multiple myeloma: a comprehensive overview. *Leukemia* **33**, 2343–2357 (2019).
7. Ledergor, G. et al. Single cell dissection of plasma cell heterogeneity in symptomatic and asymptomatic myeloma. *Nat. Med.* **24**, 1867–1876 (2018).
8. Orlowski, R. Z. et al. Carfilzomib-dexamethasone versus bortezomib-dexamethasone in relapsed or refractory multiple myeloma: updated overall survival, safety, and subgroups. *Clin. Lymphoma Myeloma Leuk.* **19**, 522–530 (2019).
9. Mateos, M. V. et al. Overall survival with daratumumab, bortezomib, melphalan, and prednisone in newly diagnosed multiple myeloma (ALCYONE): a randomised, open-label, phase 3 trial. *Lancet* **395**, 132–141 (2020).
10. Facon, T. et al. Daratumumab, lenalidomide, and dexamethasone versus lenalidomide and dexamethasone alone in newly diagnosed multiple myeloma (MAIA): overall survival results from a randomised, open-label, phase 3 trial. *Lancet Oncol.* **22**, 1582–1596 (2021).
11. Lannes, R. et al. In multiple myeloma, high-risk secondary genetic events observed at relapse are present from diagnosis in tiny, undetectable subclonal populations. *J. Clin. Oncol.* **41**, 2101987 (2022).
12. Ghosh, N., Ye, X., Ferguson, A., Huff, C. A. & Borrello, I. Bortezomib and thalidomide, a steroid free regimen in newly diagnosed patients with multiple myeloma. *Br. J. Haematol.* **152**, 593–599 (2011).
13. Branagan, A., Lei, M., Lou, U. & Raje, N. Current treatment strategies for multiple myeloma. *JCO Oncol. Pract.* **16**, 5–14 (2020).
14. Mohan, M., Hari, P. & Dhakal, B. Immunotherapy in multiple myeloma-time for a second major paradigm shift. *JCO Oncol. Pract.* **17**, 405–413 (2021).
15. Derynck, R., Turley, S. J. & Akhurst, R. J. TGFβ biology in cancer progression and immunotherapy. *Nat. Rev. Clin. Oncol.* **18**, 9–34 (2020).
16. Ciardiello, D., Elez, E., Tabernero, J. & Seoane, J. Clinical development of therapies targeting TGFβ: current knowledge and future perspectives. *Ann. Oncol.* **31**, 1336–1349 (2020).
17. Heldin, C. H. & Moustakas, A. Signaling receptors for TGF-β family members. *Cold Spring Harb. Perspect. Biol.* **8**, a022053 (2016).
18. Coskun, H. S. I. et al. Serum transforming growth factor beta 1 levels in multiple myeloma patients. *Turk. J. Hematol.* **23**, 47–52 (2006).
19. Kim, B. G., Malek, E., Choi, S. H., Ignatz-Hoover, J. J. & Driscoll, J. J. Novel therapies emerging in oncology to target the TGF-β pathway. *J. Hematol. Oncol.* **14**, 55 (2021).
20. Jung, S. Y. et al. Population pharmacokinetics of vactosertib, a new TGF-β receptor type I inhibitor, in patients with advanced solid tumors. *Cancer Chemother. Pharmacol.* **85**, 173–183 (2020).
21. Yang, L., Pang, Y. & Moses, H. L. TGF-β and immune cells: an important regulatory axis in the tumor microenvironment and progression. *Trends Immunol.* **31**, 220–227 (2010).
22. Metropulos, A. E., Munshi, H. G. & Principe, D. R. The difficulty in translating the preclinical success of combined TGFβ and immune checkpoint inhibition to clinical trial. *EBioMedicine* **86**, 104380 (2022).
23. Batlle, E. & Massagué, J. Transforming growth factor-β signaling in immunity and cancer. *Immunity* **50**, 924–940 (2019).
24. Principe, D. R. et al. TGF-β: duality of function between tumor prevention and carcinogenesis. *J. Natl Cancer Inst.* **106**, djt369 (2014).
25. Son, J. Y. et al. EW-7197, a novel ALK-5 kinase inhibitor, potently inhibits breast to lung metastasis. *Mol. Cancer Ther.* **13**, 1704–1716 (2014).
26. Hong, E. et al. Combination treatment of T1-44, a PRMT5 inhibitor with vactosertib, an inhibitor of TGF-β signaling, inhibits invasion and prolongs survival in a mouse model of pancreatic tumors. *Cell Death Dis.* **14**, 93 (2023).
27. Yoon, J. H. et al. Activin receptor-like kinase5 inhibition suppresses mouse melanoma by ubiquitin degradation of Smad4, thereby derepressing eomesodermin in cytotoxic T lymphocytes. *EMBO Mol. Med.* **5**, 1720–1739 (2013).
28. Kumar, S. et al. International Myeloma Working Group consensus criteria for response and minimal residual disease assessment in multiple myeloma. *Lancet Oncol.* **17**, e328–e346 (2016).
29. Harrold, J. M. & Abraham, A. K. Ubiquity: a framework for physiological/mechanism-based pharmacokinetic/pharmacodynamic model development and deployment. *J. Pharmacokinet. Pharmacodyn.* **41**, 141–151 (2014).
30. Jung, S. Y. et al. Pharmacokinetic characteristics of vactosertib, a new activin receptor-like kinase 5 inhibitor, in patients with advanced solid tumors in a first-in-human phase 1 study. *Investig. N. Drugs* **38**, 812–820 (2020).
31. Jung, M. et al. Safety and efficacy of vactosertib, a TGF-βR1 kinase inhibitor, in combination with paclitaxel in patients with metastatic gastric adenocarcinoma. *Ann. Oncol.* **31**, S912–1453P (2020).
32. Richardson, P. G. et al. Pomalidomide alone or in combination with low-dose dexamethasone in relapsed and refractory multiple myeloma: a randomized phase 2 study. *Blood* **123**, 1826–1832 (2014).
33. Liu, J. et al. ERK signaling mediates resistance to immunomodulatory drugs in the bone marrow microenvironment. *Sci. Adv.* **7**, eabg2697 (2021).
34. Lee, M. K. et al. TGF-beta activates Erk MAP kinase signalling through direct phosphorylation of ShcA. *EMBO J.* **26**, 3957–3967 (2007).
35. Quach, H. et al. Mechanism of action of immunomodulatory drugs (IMiDS) in multiple myeloma. *Leukemia* **24**, 22–32 (2010).

36. Lu, G. et al. The myeloma drug lenalidomide promotes the cereblon-dependent destruction of Ikaros proteins. *Science* **343**, 305–309 (2014).
37. Oh, S. A. & Li, M. O. TGF-β: guardian of T cell function. *J. Immunol.* **191**, 3973–3979 (2013).
38. Sacher, A. G. & Gandhi, L. Biomarkers for the clinical use of PD-1/PD-L1 inhibitors in non–small-cell lung cancer: a review. *JAMA Oncol.* **2**, 1217–1222 (2016).
39. Wolf, Y., Anderson, A. C. & Kuchroo, V. K. TIM3 comes of age as an inhibitory receptor. *Nat. Rev. Immunol.* **20**, 173–185 (2020). TIM-3.
40. Walunas, T. L. et al. CTLA-4 can function as a negative regulator of T cell activation. *Immunity* **1**, 405–413 (1994).
41. Pardoll, D. The blockade of immune checkpoints in cancer immunotherapy. *Nat. Rev. Cancer* **12**, 252–264 (2012).
42. Liu, Z. et al. Study on Tim3 regulation of multiple myeloma cell proliferation via NF-κB signal pathways. *Front. Oncol.* **10**, 584530 (2020).
43. Colak, S. & Ten Dijke, P. Targeting TGFβ signaling in cancer. *Trends Cancer* **3**, 56–71 (2017).
44. Rich, S., Seelig, M., Lee, H. M. & Lin, J. Transforming growth factor beta 1 co-stimulated growth and regulatory function of staphylococcal enterotoxin B-responsive CD8+ T cells. *J. Immunol.* **155**, 609–618 (1995).
45. Richardson, P. G., HORIZON (OP-106) Investigators et al. Melflufen and dexamethasone in heavily pretreated relapsed and refractory multiple myeloma. *J. Clin. Oncol.* **39**, 757–767 (2021).
46. Miguel, J. S. et al. Pomalidomide plus low-dose dexamethasone versus high-dose dexamethasone alone for patients with relapsed and refractory multiple myeloma (MM-003): a randomised, open-label, phase 3 trial. *Lancet Oncol.* **14**, 1055–1066 (2013).
47. Chari, A. et al. Oral selinexor-dexamethasone for triple-class refractory multiple myeloma. *N. Engl. J. Med.* **381**, 727–738 (2019).
48. Rana, P. S., Soler, D. C., Kort, J. & Driscoll, J. J. Targeting TGF-β signaling in the multiple myeloma microenvironment: steering CARs and T cells in the right direction. *Front. Cell Dev. Biol.* **10**, 1059715 (2022).
49. Aref, S., Azmy, E. & El-Gilany, A. H. Upregulation of CD200 is associated with regulatory T cell expansion and disease progression in multiple myeloma. *Hematol. Oncol.* **35**, 51–57 (2017).
50. Kröning, H. et al. Overproduction of IL-7, IL-10 and TGF-beta 1 in multiple myeloma. *Acta Haematol.* **98**, 116–118 (1997).
51. Musto, P., International Myeloma Working Group et al. Second primary malignancies in multiple myeloma: an overview and IMWG consensus. *Ann. Oncol.* **28**, 228–245 (2017).
52. LiverTox: Clinical and Research Information on Drug-Induced Liver Injury [Internet]. Bethesda (MD): National Institute of Diabetes and Digestive and Kidney Diseases; 2012–. Pomalidomide. [Updated 2022 Aug 30]. Available from: https://www.ncbi.nlm.nih.gov/books/NBK548343/.
53. Dooley, S. & ten Dijke, P. TGF-β in progression of liver disease. *Cell Tissue Res.* **347**, 245–256 (2012).
54. Platzbecker, E. et al. Efficacy and safety of luspatercept versus epoetin alfa in erythropoiesis-stimulating agent-naïve, transfusion-dependent lower-risk myelodysplastic syndromes. *Lancet* **402**, 373–385 (2023).
55. Sher, T. et al. A steroid-independent regimen of bortezomib, liposomal doxorubicin and thalidomide demonstrate high response rates in newly diagnosed multiple myeloma patients. *Br. J. Haematol.* **154**, 104–110 (2011).
56. Petrelli, F. et al. Association of steroids use with survival in patients treated with immune checkpoint inhibitors: a systematic review and meta-analysis. *Cancers* **27**, 546 (2020).
57. Jagannath, S. et al. Bortezomib in recurrent and/or refractory multiple myeloma: initial clinical experience in patients with impaired renal function. *Cancer Interdiscip. Int. J. Am. Cancer. Soc.* **103**, 1195–1200 (2005).
58. San-Miguel, J. F. et al. Efficacy and safety of bortezomib in patients with renal impairment: results from the APEX phase 3 study. *Leukemia* **22**, 842–849 (2008).
59. Rajkumar, S. V. et al. Multicenter, randomized, double-blind, placebo-controlled study of thalidomide plus dexamethasone compared with dexamethasone as initial therapy for newly diagnosed multiple myeloma. *J. Clin. Oncol.* **26**, 2171–2177 (2008).
60. Thomas, D. A. & Massagué, J. TGF-β directly targets cytotoxic T cell functions during tumor evasion of immune surveillance. *Cancer Cell* **8**, 369–380 (2005).
61. Hideshima, T., Mitsiades, C., Tonon, G., Richardson, P. G. & Anderson, K. C. Understanding multiple myeloma pathogenesis in the bone marrow to identify new therapeutic targets. *Nat. Rev. Cancer* **7**, 585–598 (2007).
62. Gorelik, L. & Flavell, R. A. Immune-mediated eradication of tumors through the blockade of transforming growth factor-beta signaling in T cells. *Nat. Med.* **7**, 1118–1122 (2001).
63. Marie, J. C., Liggitt, D. & Rudensky, A. Y. Cellular mechanisms of fatal early-onset autoimmunity in mice with the T cell-specific targeting of transforming growth factor-β receptor. *Immunity* **25**, 441–454 (2006).
64. Tumeh, P. C. et al. PD-1 blockade induces responses by inhibiting adaptive immune resistance. *Nature* **515**, 568–571 (2014).
65. Ribas, A. & Wolchok, J. D. Cancer immunotherapy using checkpoint blockade. *Science* **359**, 1350–1355 (2018).
66. Li, H. et al. Dysfunctional CD8 T cells form a proliferative, dynamically regulated compartment within human melanoma. *Cell* **176**, 775–789 (2019).
67. Grenga, I. et al. Anti-PD-L1/TGFβR2 (M7824) fusion protein induces immunogenic modulation of human urothelial carcinoma cell lines, rendering them more susceptible to immune-mediated recognition and lysis. *Urol. Oncol.* **36**, 93.e1–93.e11 (2018).
68. Amaria, R. N. et al. Neoadjuvant relatlimab and nivolumab in resectable melanoma. *Nature* **611**, 155–160 (2022).
69. Dodagatta-Marri, E. et al. α-PD-1 therapy elevates Treg/Th balance and increases tumor cell pSmad3 that are both targeted by α-TGFβ antibody to promote durable rejection and immunity in squamous cell carcinomas. *J. Immunother. Cancer* **7**, 62 (2019).
70. Munshi, N. C. et al. Idecabtagene vicleucel in relapsed and refractory multiple myeloma. *N. Engl. J. Med.* **384**, 705–716 (2021).
71. Berdeja, J. G. et al. Ciltacabtagene autoleucel, a B-cell maturation antigen-directed chimeric antigen receptor T-cell therapy in patients with relapsed or refractory multiple myeloma (CARTITUDE-1): a phase 1b/2 open-label study. *Lancet* **398**, 314–324 (2021).
72. Mailankody, S. et al. GPRC5D-targeted CAR T cells for myeloma. *N. Engl. J. Med.* **387**, 1196–1206 (2022).
73. Rana, P. S., Murphy, E. V., Kort, J. & Driscoll, J. J. Road testing new CAR design strategies in multiple myeloma. *Front. Immunol.* **13**, 957157 (2022).
74. Scudiero, D. A. et al. Evaluation of a soluble tetrazolium/formazan assay for cell growth and drug sensitivity in culture using human and other tumor cell lines. *Cancer Res.* **48**, 4827–4833 (1988).


## Acknowledgements

Research was supported by NIH R01 (5R01AI139141 to J.J.D.), University Hospitals Cleveland Medical Center, Seidman Cancer Center, the Vinney Foundation (J.J.D.) and the Case Comprehensive Cancer Center (to J.J.D.). This research was also supported by the Translational Research Shared Resources of the Case Comprehensive Cancer Center (P30 CA#43703). The authors also state that the Life Technologies Attune NxT Flow Cytometer was acquired through an NIH Shared Instrumentation Grant and, as such, we are required by NIH Regulations to specifically cite the assistance of the Case Comprehensive Cancer Center Cytometry & Microscopy Shared Resource and NIH Grant S10-NIH OD021559. The investigators initiated and designed the trial, collected

and had full and unrestricted access to the data, and performed the final analysis. Medpacto provided the study drug but had no role in study design, data collection, analysis or interpretation.

## Author contributions

E. Ma. and J.J.D. developed the concept. E. Ma., P.S.R,. M.S., E. Mu., M.D., J.I.H., M.M., L.M., S.J.K. and J.J.D. analyzed the data. E. Ma., J.J.D., P.S.R. and J.I.H. wrote the initial version of the manuscript and edited subsequent versions. All authors made substantial contributions and approved the final version of the manuscript.

## Competing interests

The authors declare no competing interests.

## Additional information

**Supplementary information** The online version contains supplementary material available at https://doi.org/10.1038/s41467-024-51442-2.

**Correspondence** and requests for materials should be addressed to Ehsan Malek or James J. Driscoll.

**Peer review information** *Nature Communications* thanks Rosemary Akhurst, Francesca Cottini and the other, anonymous, reviewer(s) for their contribution to the peer review of this work. A peer review file is available.

**Reprints and permissions information** is available at http://www.nature.com/reprints

**Publisher's note** Springer Nature remains neutral with regard to jurisdictional claims in published maps and institutional affiliations.



[1]Adult Hematologic Malignancies & Stem Cell Transplant Section, Seidman Cancer Center, University Hospitals Cleveland Medical Center, Cleveland, OH, USA. [2]Division of Hematology Oncology, Case Western Reserve University School of Medicine, Cleveland, OH, USA. [3]Case Comprehensive Cancer Center, Case Western Reserve University, Cleveland, OH, USA. [4]Department of Pharmacology, Case Western Reserve University School of Medicine, Cleveland, OH, USA. [5]Center for Proteomics and Bioinformatics, Case Western Reserve University School of Medicine, Cleveland, OH, USA. [6]Department of Biochemistry, Case Western Reserve University School of Medicine, Cleveland, OH, USA. [7]Medpacto Inc., Seoul, Republic of Korea.
✉e-mail: ehsan.malek@RoswellPark.org; james.driscoll@UHhospitals.org